iScience

CellPress

Article

# Coxsackievirus B Persistence Modifies the Proteome and the Secretome of Pancreatic Ductal Cells

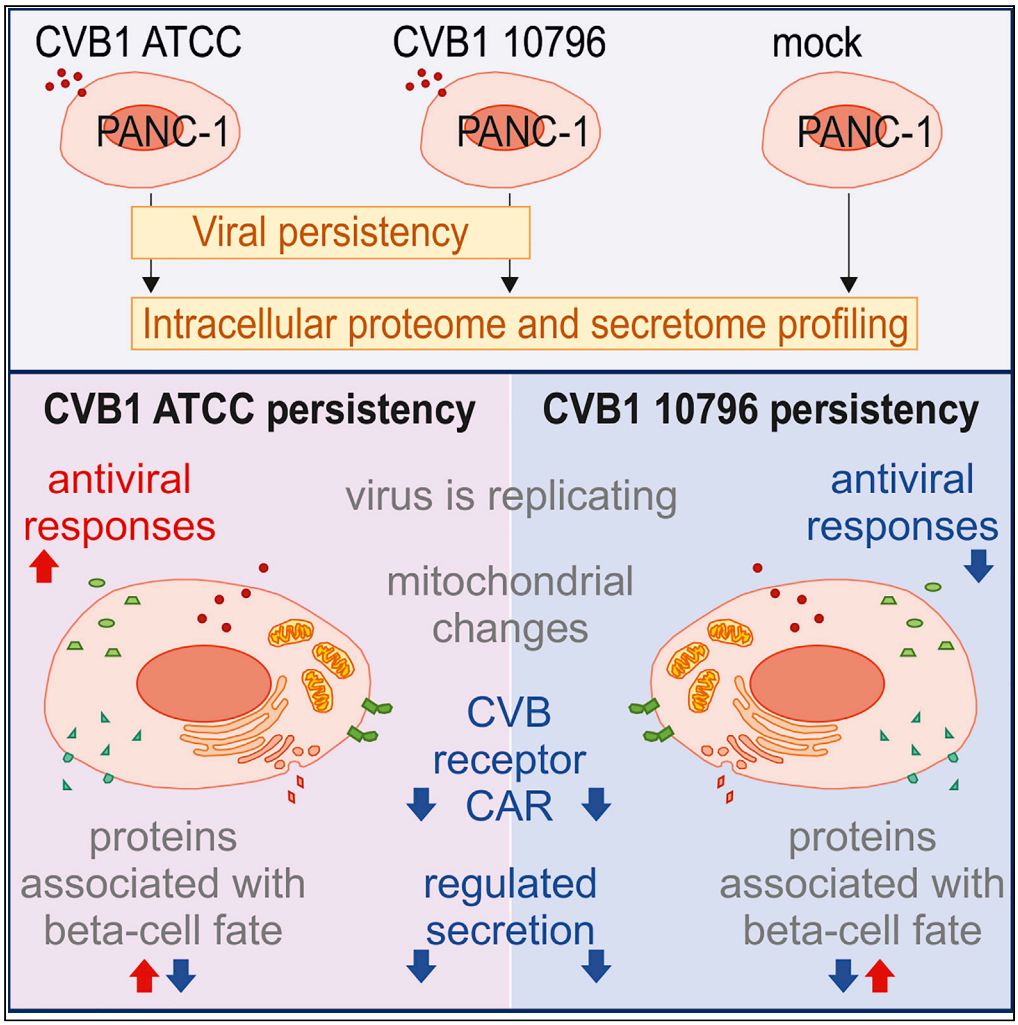


Niina Lietzén, Karoliina Hirvonen, Anni Honkimaa, ..., Amir-Babak Sioofy-Khojine, Heikki Hyöty, Riitta Lahesmaa

riitta.lahesmaa@utu.fi

## HIGHLIGHTS

Persistent CVB infection in PANC-1 cells established using two CVB1 strains

Infections influenced host protein expression and secretion broadly

Changes in, e.g., mitochondria, virus receptors, and regulated secretory pathway

Persistency-triggered antiviral immune responses differed between the virus strains

## DATA AND CODE AVAILABILITY

PXD012153
PXD012154

Lietzén et al., iScience 19, 340–357
September 27, 2019 
https://doi.org/10.1016/j.isci.2019.07.040

iScience

CellPress

Article

# Coxsackievirus B Persistence Modifies the Proteome and the Secretome of Pancreatic Ductal Cells

Niina Lietzén,[1,6] Karoliina Hirvonen,[1,6] Anni Honkimaa,[2,6] Tanja Buchacher,[1] Jutta E. Laiho,[2] Sami Oikarinen,[2] Magdalena A. Mazur,[3] Malin Flodström-Tullberg,[3] Eric Dufour,[4] Amir-Babak Sioofy-Khojine,[2] Heikki Hyöty,[2,5,7] and Riitta Lahesmaa[1,7,8,*]

## SUMMARY

**The group B Coxsackieviruses (CVB), belonging to the *Enterovirus* genus, can establish persistent infections in human cells. These persistent infections have been linked to chronic diseases including type 1 diabetes. Still, the outcomes of persistent CVB infections in human pancreas are largely unknown. We established persistent CVB infections in a human pancreatic ductal-like cell line PANC-1 using two distinct CVB1 strains and profiled infection-induced changes in cellular protein expression and secretion using mass spectrometry-based proteomics. Persistent infections, showing characteristics of carrier-state persistence, were associated with a broad spectrum of changes, including changes in mitochondrial network morphology and energy metabolism and in the regulated secretory pathway. Interestingly, the expression of antiviral immune response proteins, and also several other proteins, differed clearly between the two persistent infections. Our results provide extensive information about the protein-level changes induced by persistent CVB infection and the potential virus-associated variability in the outcomes of these infections.**

## INTRODUCTION

Enteroviruses are the most common human viruses, causing a wide spectrum of diseases ranging from mild common cold-type illness to severe life-threatening conditions. Polioviruses causing paralytic diseases are their most well-known representatives (Laitinen et al., 2016). The group B Coxsackieviruses (CVBs) are among those enteroviruses that most frequently lead to contacts with the health care system causing, e.g., meningitis, encephalitis, myocarditis, hand-foot-and-mouth disease, pancreatitis, and hepatitis (Tapparel et al., 2013). Young children are at the highest risk of developing severe CVB diseases, and infection in newborn infants can lead to life-threatening systemic infections. CVB infections are typically acute, and the host's immune system clears the virus within a few days or weeks. CVBs can, however, also establish chronic (persistent) infections (Chapman and Kim, 2008; Pinkert et al., 2011; Sane et al., 2013), which have been linked to chronic diseases including type 1 diabetes (T1D) and dilated cardiomyopathy (Nurminen et al., 2012; Massilamany et al., 2014; Hyoty, 2016).

CVBs are small, non-enveloped viruses, and their positive-sense single-stranded RNA genome is inside the icosahedral protein capsid (Tuthill et al., 2010). There are six different CVB serotypes (CVB1–6) that can be separated from each other based on their antigenic and genetic properties. The viral genome encodes for viral structural proteins, VP1–4, and seven non-structural proteins, 2A–2C and 3A–3D. The infection cycle starts by the attachment of the virus to the cell surface receptor followed by viral entry into the cell (Tuthill et al., 2010). The viral RNA genome is released by uncoating and is transported into the cytoplasm where it is transcribed and translated. Finally, mature virions are released, usually by lysis of infected cells (Laitinen et al., 2016).

The mechanisms leading to enteroviral persistency are not fully understood. However, it appears that the development of viral persistency is linked to a complex co-evolutionary process of both the host cell and the virus (Alidjinou et al., 2017; Pinkert et al., 2011). Studies in cell and animal models suggest that there are two types of persistent infections, called carrier-state and steady-state persistence. In a steady-state infection the viral replication cycle is non-lytic and a large proportion of cells can be simultaneously infected (Frisk, 2001). In a carrier-state infection high titers of virus are produced, but only a small proportion of

[1]Turku Bioscience Centre, University of Turku and Åbo Akademi University, FI-20520 Turku, Finland

[2]Faculty of Medicine and Health Technology, Tampere University, FI-33014 Tampere, Finland

[3]Center for Infectious Medicine, Department of Medicine Huddinge, Karolinska Institutet, Karolinska University Hospital, Stockholm 141 86, Sweden

[4]Faculty of Medicine and Life Sciences, BioMediTech Institute and Tampere University Hospital, FI-33014 Tampere, Finland

[5]Fimlab Laboratories, Pirkanmaa Hospital District, FI-33520 Tampere, Finland

[6]These authors contributed equally

[7]These authors contributed equally

[8]Lead Contact

*Correspondence: riitta.lahesmaa@utu.fi

https://doi.org/10.1016/j.isci.2019.07.040

 

the cells are infected (Alidjinou et al., 2017; Pinkert et al., 2011). Kim et al. have established a steady-state infection with CVB3 in primary cells isolated from different tissues including human cardiac myocytes and mouse heart and pancreatic cells (Kim et al., 2008). Infection did not cause cell lysis, even though viral RNA was produced. However, the viral genome harbored 7- to 49-nucleotide-long deletions in the untranslated region in the 5′ end (Kim et al., 2008), which may explain the non-lytic character of the virus. Carrier-state CVB3 infection has been established in murine cardiac myocyte cell line, HL-1 (Pinkert et al., 2011). Another carrier-state infection model has been established in pancreatic duct cell line, PANC-1, using CVB4 (Sane et al., 2013). The viral plaque morphology changed, and several mutations accumulated in the viral genome during the development of persistent infection. The persistently infected cells also became resistant to the cytopathic effect induced by CVB4 re-infection (Alidjinou et al., 2017). The CVB receptor coxsackievirus and adenovirus receptor (CXADR) was downregulated in these carrier-state models, which may contribute to the resistance of persistently infected cells to superinfection by other CVBs and to the lack of fulminant cytopathic effect (Alidjinou et al., 2017; Pinkert et al., 2011). Finally, previous studies have suggested that individual strains of a given CVB type can differ in their effects on target cells and in their ability to induce antiviral host responses (Anagandula et al., 2014; Hamalainen et al., 2014; Ylipaasto et al., 2012). Such differences might also influence how efficiently the infection is eradicated and the persistence of the virus in the infected cells or organs.

Pancreas is an important target organ of CVBs, which can infect both exocrine and endocrine cells of human pancreas (Busse et al., 2017; Richardson et al., 2009). A role for CVBs in the pathogenesis of T1D is supported by the strong expression of CXADR in insulin-producing pancreatic beta-cells (Ifie et al., 2018) because CVBs, but no other enteroviruses, use this receptor to enter the cell. Enterovirus VP1 protein has been repeatedly detected in the beta-cells of patients with T1D (Krogvold et al., 2015; Richardson et al., 2009, 2013). However, only few beta-cells express viral protein and the amount of viral RNA is low, consistent with a low-grade viral persistence rather than an acute productive infection. CVBs have also occasionally been detected outside of pancreatic islets in human pancreas tissue samples (Busse et al., 2017; Richardson et al., 2009; Ylipaasto et al., 2004). Interestingly, a small set of data based on a novel and sensitive approach for detecting CVB RNA indicated the presence of these viruses outside pancreatic islets also in tissue biopsies collected from individuals with T1D (Busse et al., 2017). The association between CVBs and T1D has been documented in prospective birth cohort studies already before the beta-cell damaging process has started (Laitinen et al., 2014; Oikarinen et al., 2014; Sioofy-Khojine et al., 2018), suggesting that these viruses can play a role in the initiation of the process. Among the six CVB types, CVB1 and CVB4 have most frequently been associated with T1D (Laitinen et al., 2014; Oikarinen et al., 2014; Sioofy-Khojine et al., 2018; Yoon et al., 1979).

The present study aims at identifying cellular responses during persistent CVB infection and understanding the mechanisms mediating the adaptation of cells to the carrier-type persistence. Establishing long-term CVB persistency in primary human pancreatic islets (Chehadeh et al., 2000) or insulin-producing beta-cell lines is challenging. Here we utilized a well-established model of persistent CVB infection in PANC-1 cells (Sane et al., 2013) for broad mapping of infection-induced changes in protein expression and secretion after almost 1 year's persistency. Persistent infections were established by using two distinct strains of CVB1, an enterovirus that has been previously associated with T1D in epidemiological studies (Laitinen et al., 2014; Oikarinen et al., 2014; Sioofy-Khojine et al., 2018). In our previous study (Hamalainen et al., 2014), these two strains differed by the strength of innate immune responses they induced. Infection-associated changes in intracellular proteomes and secretomes were profiled using quantitative mass spectrometry-based proteomics.

## RESULTS

### Coxsackievirus B1 ATCC and 10796 Strains Establish Persistent Infections in PANC-1 Cells

Persistent CVB1 infection was established in the PANC-1 human pancreatic duct cell line using two virus strains (ATCC and 10796). We observed a strong cytopathic effect immediately after the initial infection with both CVB strains, and the amount of viral RNA in cell culture supernatants, measured by RT-qPCR, dropped dramatically at this point, likely due to the rapid loss of cells that could support viral replication. Restored proliferation in the surviving cells was associated with an increased amount of viral RNA reaching, in both models, $10^8$ copies per sample approximately 3 months after the initial infection (Figure 1A). Thereafter, the copy number of viral RNA remained stable. Around a year after the initial infection, the viral capsid protein VP1 was detected by immunohistochemical (IHC) staining (Figure 1B), and both established models

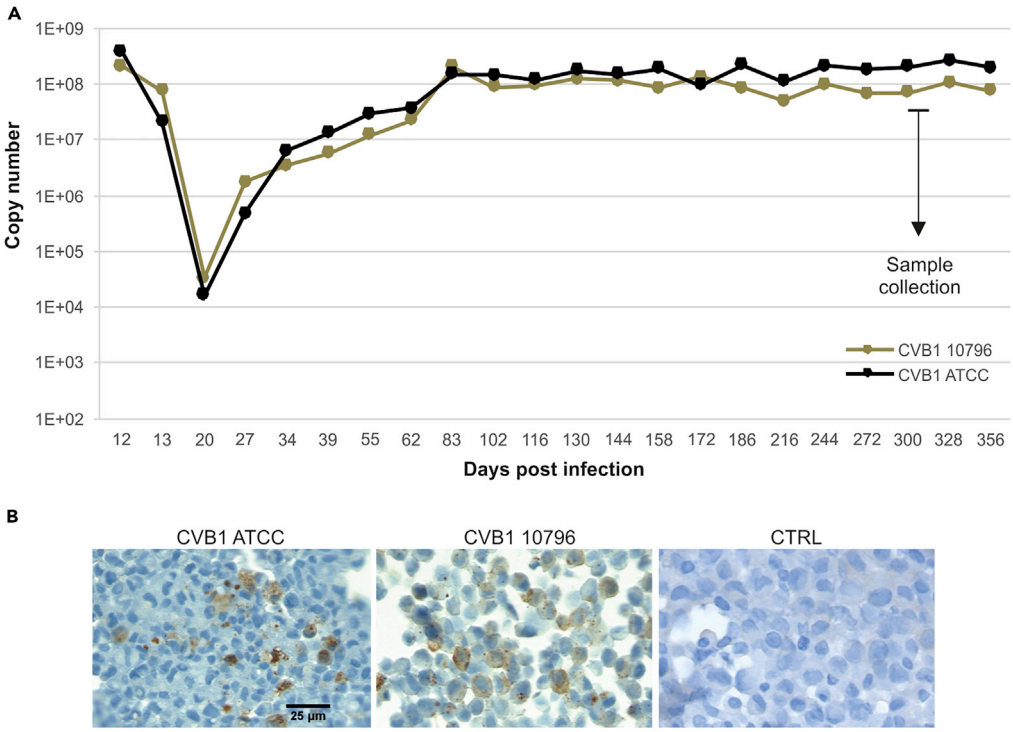


**Figure 1. Establishment of Persistent CVB1 Infections in PANC-1 Cells**

(A) Both CVB1 strains (ATCC and 10796) were replicating in PANC-1 cells for nearly 1 year. The amount of viral RNA was measured by RT-qPCR, and the results were converted into genome copy numbers/sample (140 µL). Sample collection for proteomics was performed 300, 315, and 322 days post-infection, as indicated in the figure.

(B) Viral capsid protein VP1 (brown) was detected by IHC at 362 days post-infection. Scale bar, 25 µm.

showed features of carrier-state persistent infection with a low proportion of the cells clearly positive for viral VP1 protein (Alidjinou et al., 2017; Pinkert et al., 2011). The proteomes of these persistently infected cells were analyzed at this time. Persistent CVB1 infections were not associated with increased cell death (Table S1).

## Persistent Coxsackievirus B1 Infection Results in Extensive Changes in Protein Expression and Secretion

Using mass spectrometry-based proteomics, we identified and quantified altogether 5,130 distinct protein groups in the cell lysates and 3,181 distinct protein groups in the cell culture supernatants of the PANC-1 cells (Tables S2 and S3). Persistent CVB1 infections were associated with extensive changes in intracellular protein expression and protein secretion. Significant upregulation of 688 distinct protein groups was observed in PANC-1 cells with persistent CVB1 infection, with 85 of the protein groups significantly upregulated in both persistent CVB1 infection models (Figures 2A and 2B). Furthermore, persistent CVB1 infections were associated with significant downregulation of 2,001 distinct protein groups in the PANC-1 cells, with 520 of the protein groups significantly downregulated in both persistent infection models (Figures 2A and 2B). Finally, significant upregulation of 919 distinct protein groups and significant downregulation of 630 distinct protein groups was observed in the cell culture supernatants of the persistent CVB1 infection models (Figure 2C). Of them, the secretion of 166 and 197 distinct protein groups was significantly upregulated and downregulated in both persistent CVB1 infection models, respectively (Figures 2C and 2D).

## Proteins Potentially Involved in Viral Replication and Spreading Were Influenced during Persistent CVB1 Infection

Downregulation of a broad spectrum of host proteins was observed in the PANC-1 cells in both persistent CVB1 infection models (Figures 2A and 2B). CVB proteinase 2A can block the host cell translational machinery and promote viral IRES-driven translation via cleavage of host translation initiation factor eIF4G

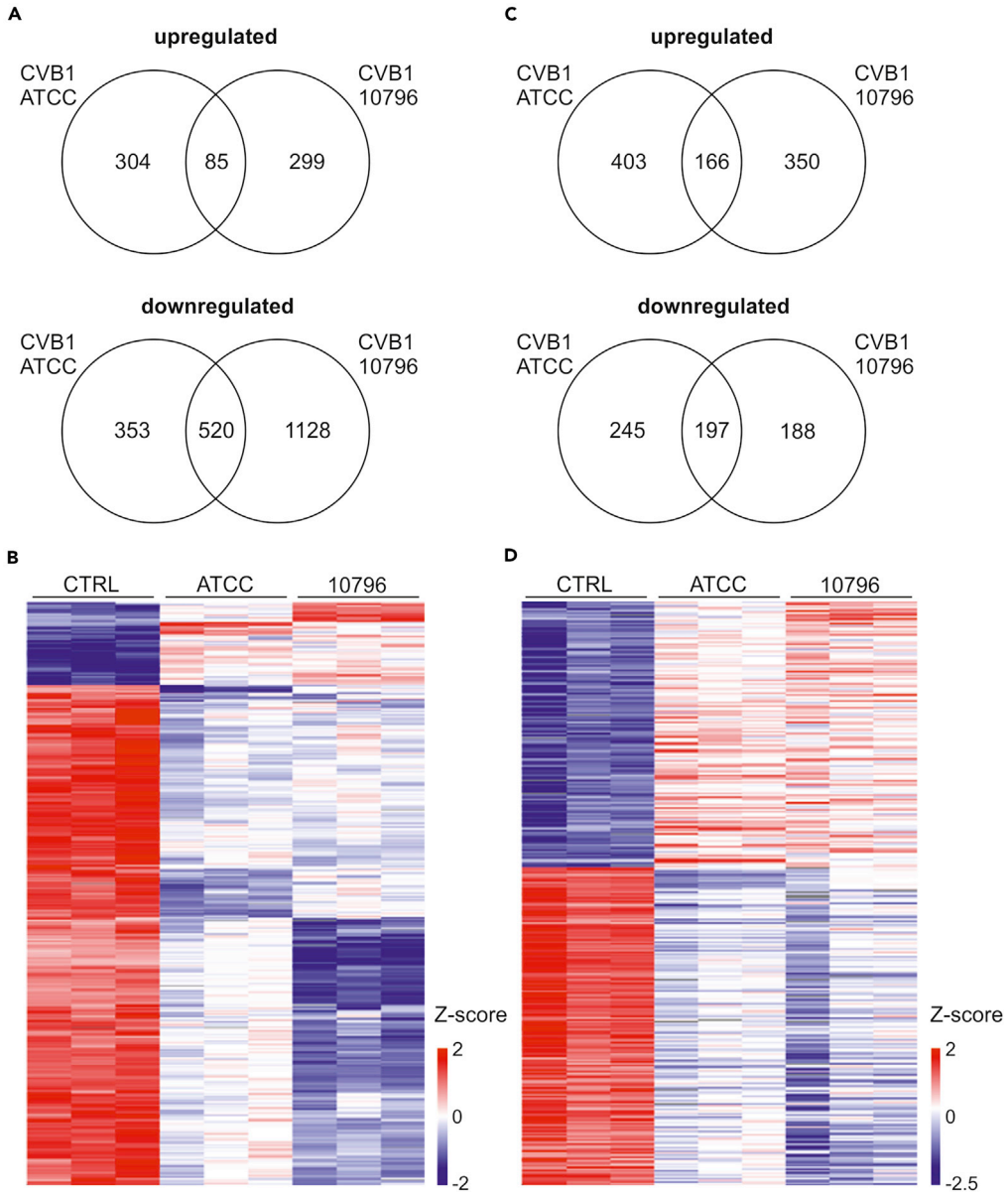


**Figure 2. Persistent CVB1 Infection Results in Changes in Intracellular Protein Expression and Protein Secretion**

(A) Numbers of differentially expressed proteins in cells with persistent CVB1 ATCC and 10796 infection.

(B) Heatmap of *Z*-score normalized data for the 605 proteins with similar responses to persistent CVB1 infection with both virus strains in the PANC-1 cells.

(C) Numbers of proteins whose secretion is significantly changed during persistent CVB1 ATCC and 10796 infections.

(D) Heatmap of *Z*-score normalized data showing the 363 proteins whose secretion is changed similarly from cells with persistent CVB1 ATCC and 10796 infections.

required for cap-dependent translation (Borman et al., 1997). Indeed, western blot analysis showed the presence of cleaved eIF4G in both persistent CVB1 infection models (Figure 3A). Based on Ingenuity Pathway Analysis (IPA), proteins involved in cholesterol biosynthesis pathways and the mevalonate pathway, which provides building blocks for cholesterol biosynthesis, were significantly enriched among the upregulated proteins in both persistent infection models (Figure 3B, Table S4). Cholesterol is known to facilitate efficient CVB replication, and CVBs manipulate host cell cholesterol shuttle to accumulate this lipid in viral replication organelles (Albulescu et al., 2015; Ilnytska et al., 2013). Poly(rC)-binding protein 2 (PCBP2) is essential for CVB IRES-mediated translation and viral RNA replication (Sean et al., 2009), and its

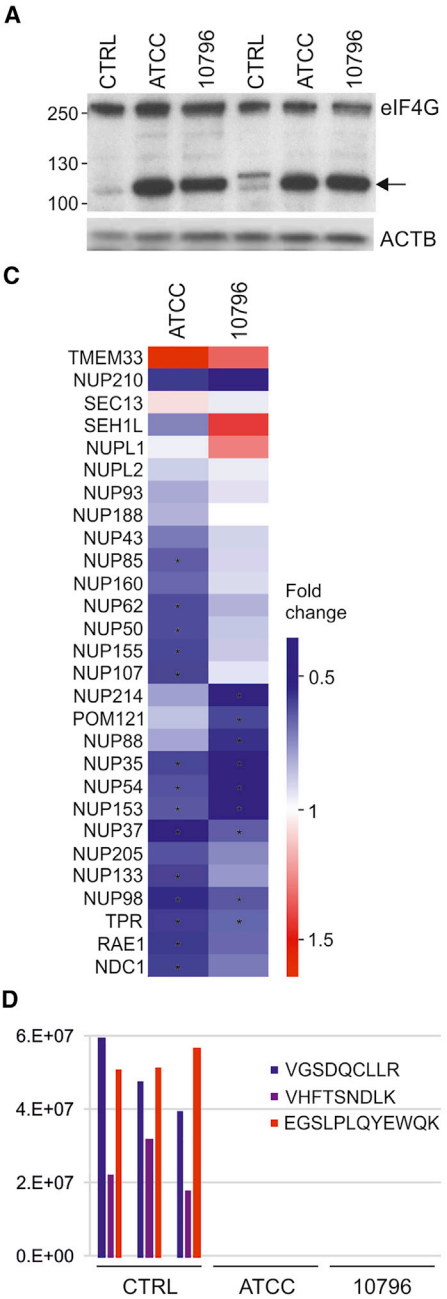


**B**

| Upregulated during ATCC and 10796 infection | p-value ATCC | p-value 10796 |
|---|---|---|
| Superpathway of Cholesterol Biosynthesis | 3.6E-8 | 6.5E-7 |
| Cholesterol Biosynthesis I | 9.5E-5 | 8.9E-5 |
| Cholesterol Biosynthesis II (via 24,25-dihydrolanosterol) | 9.5E-5 | 8.9E-5 |
| Cholesterol Biosynthesis III (via Desmosterol) | 9.5E-5 | 8.9E-5 |
| Superpathway of Geranylgeranyldiphosphate Biosynthesis I (via Mevalonate) | 2.3E-4 | 3.4E-3 |
| 14-3-3-mediated Signaling | 2.8E-4 | 4.9E-5 |
| Remodeling of EpithelialAdherens Junctions | 3.3E-4 | 4.8E-9 |
| NRF2-mediated Oxidative Stress Response | 4.4E-4 | 4.2E-3 |
| Huntington's Disease Signaling | 4.6E-4 | 9.3E-3 |
| Breast Cancer Regulation by Stathmin1 | 8.3E-4 | 5.5E-7 |
| Mevalonate Pathway I | 1.5E-3 | 1.4E-3 |
| Arginine Biosynthesis IV | 5.6E-3 | 5.4E-3 |
| Arginine Degradation VI (Arginase 2 Pathway) | 5.6E-3 | 5.4E-3 |
| Proline Biosynthesis II (from Arginine) | 5.6E-3 | 5.4E-3 |
| Germ Cell-Sertoli Cell Junction Signaling | 6.8E-3 | 1.2E-4 |
| Sertoli Cell-Sertoli Cell Junction Signaling | 7.9E-3 | 2.1E-3 |

**E**

| Downregulated during ATCC and 10796 infection | p-value ATCC | p-value 10796 |
|---|---|---|
| Mitochondrial Dysfunction | 6.3E-15 | 2.0E-27 |
| Oxidative Phosphorylation | 5.0E-14 | 1.3E-18 |
| Leucine Degradation I | 5.5E-7 | 2.6E-5 |
| Valine Degradation I | 6.6E-6 | 7.9E-11 |
| Sirtuin Signaling Pathway | 2.2E-5 | 3.2E-21 |
| Aldosterone Signaling in Epithelial Cells | 5.0E-5 | 1.0E-3 |
| Aryl Hydrocarbon Receptor Signaling | 1.1E-4 | 2.1E-4 |
| Phagosome Maturation | 1.3E-4 | 2.3E-10 |
| Chondroitin Sulfate Degradation (Metazoa) | 2.4E-4 | 4.8E-3 |
| Huntington's Disease Signaling | 2.6E-4 | 6.9E-5 |
| Histamine Degradation | 3.5E-4 | 1.1E-5 |
| NRF2-mediated Oxidative Stress Response | 7.8E-4 | 1.8E-6 |
| Fatty Acid a-oxidation | 8.9E-4 | 5.8E-5 |
| Fatty Acid ß-oxidation I | 1.7E-3 | 2.5E-11 |
| Virus Entry via Endocytic Pathways | 1.8E-3 | 2.4E-3 |
| TCA Cycle II (Eukaryotic) | 2.9E-3 | 8.5E-6 |
| Oxidative Ethanol Degradation III | 5.6E-3 | 3.5E-5 |
| Docosahexaenoic Acid (DHA) Signaling | 7.6E-3 | 4.1E-3 |
| Germ Cell-Sertoli Cell Junction Signaling | 8.1E-3 | 2.5E-3 |
| Putrescine Degradation III | 8.7E-3 | 6.8E-4 |
| Paxillin Signaling | 9.3E-3 | 4.9E-5 |

**Figure 3. Both Persistent CVB1 Infections Modulate the Expression of Multiple Host Cell Proteins**

(A) eIF4G is cleaved in PANC-1 cells with persistent CVB1 ATCC and 10796 infection. Western blot analyses were performed for two biological replicates from each condition.

(B) IPA canonical pathways that are significantly enriched among the upregulated proteins in both persistent CVB1 infection models.

(C) Several nuclear complex proteins are downregulated during persistent CVB1 infection. Nuclear pore complex proteins were assigned based on Knockenhauer and Schwartz (2016). *FDR < 0.05 and |Fold change| ≥ 1.5.

(D) Raw intensities of three CXADR peptides in the PANC-1 cells. For each sample, median intensity of three technical replicates is shown.

(E) IPA canonical pathways that are significantly enriched among the downregulated proteins in both persistent CVB1 infection models. FDR, false discovery rate.

expression was significantly upregulated in both persistent CVB1 infection models (Table S2). In addition to PCBP2, other host RNA-binding proteins also can improve the replication of CVB viruses. Interfering with the cell's nucleocytoplasmic trafficking can hinder the transport of these proteins from the cytoplasm to the nucleus making them more accessible for the virus replicating in the cytoplasm (Belov et al., 2000; Gustin

and Sarnow, 2001). In the current study, several proteins of the nuclear pore complex responsible for protein nucleocytoplasmic trafficking were significantly downregulated in both persistent infection models (Figure 3C).

Several viral peptides were identified in the cells and the cell culture supernatants of the persistent CVB1 infection models, supporting the presence of actively replicating virus still more than 300 days after the initial infection (Table S5). Interestingly, higher expression of viral proteins was detected in the cells and the cell culture supernatants during persistent infection with 10796 strain of CVB1 when compared with CVB1 ATCC infection model (Table S5). Here, the viral protein expression in each sample was defined as the sum of intensities for peptides mapping to genome polyprotein sequence of CVB1 Japan strain (UniProtKB: P08291), which is the only manually curated CVB1 protein sequence available in the SwissProt database.

Downregulation of the CVB receptor CXADR has been a common feature for carrier-state persistent CVB infections (Alidjinou et al., 2017; Pinkert et al., 2011). In line with these studies, CXADR protein expression was only detected in the non-infected PANC-1 cells (Figure 3D, Table S2), suggesting its downregulation during persistent CVB1 infection. However, neither of the persistent CVB1 virus strains lose their ability to use CXADR receptor in the entry, because they infected CAR-transfected CHO cells but were unable to infect naive CHO cells (data not shown). Furthermore, proteins involved in virus entry via the endocytic pathways were enriched among the downregulated proteins in both persistent infection models based on IPA analysis (Figure 3E, Table S4), indicating also a broader downregulation of proteins potentially involved in viral entry during persistent CVB1 infection. These changes are likely to limit the spreading of the virus from cell to cell during persistent infection.

### Persistent CVB1 Infections Are Associated with Changes in Mitochondrial Energy Metabolism and Network Morphology

One of the main features of the persistent CVB1 infection models was the significant downregulation of mitochondrial proteins, especially those proteins involved in mitochondrial energy metabolism (Figure 3E, Tables S4 and S6). Downregulation of mitochondrial energy metabolism has earlier been observed in mouse models of cardiomyopathy associated with chronic CVB3 infection (Nishtala et al., 2011; Xu et al., 2011). Mitochondrial oxidative phosphorylation was among the three most significantly downregulated pathways in both persistent infection models (Figure 3E) with 27 and 42 oxidative phosphorylation chain components downregulated by ATCC and 10796 strains of CVB1, respectively. In addition, for example, pathways of fatty acid beta-oxidation, citric acid cycle, and leucine and valine degradation were significantly enriched among the downregulated proteins in both models (Figure 3E, Table S4).

To get a deeper view on persistent CVB1 infection-induced mitochondrial changes, mitochondrial networks in the PANC-1 cells were visualized using MitoTracker staining, which labels active mitochondria based on mitochondrial membrane potential (Figure 4A). Mitochondrial network morphology is highly responsive to the existing conditions and influences cellular metabolism and several other signaling pathways (Wai and Langer, 2016). The stained cells were subdivided into four different categories based on the morphology of their mitochondrial network: elongated filaments, filaments, intermediate, and fragmented network. A high proportion (44% $\pm$ 14%, $p < 0.01$) of the cells persistently infected with 10796 strain of CVB1 showed fragmented mitochondrial network, whereas the majority of the uninfected control cells and cells infected with the ATCC strain of CVB1 showed filamentous networks (Figure 4B). Further supporting these results, proteomics analyses showed the significant downregulation of three proteins with central roles in mitochondrial fusion processes, namely, mitofusin 1, mitofusin 2 (MFN1 and MFN2), and dynamin-like 120-kDa mitochondrial protein (OPA1) (Wai and Langer, 2016), in the CVB1 10796 persistent infection model.

### Classical and Unconventional Protein Secretion from PANC-1 Cells Is Modulated by Persistent CVB1 Infection

Persistent CVB1 infections changed significantly the secretion of 1,483 proteins from the PANC-1 cells. Of these, 623 proteins were associated with extracellular exosomes based on their Gene Ontology annotations (Table S6), indicating that they might be secreted from the cells by unconventional vesicle-mediated mechanisms. The tetraspanin family of proteins is highly enriched in the membranes of exosomes (Andreu and Yáñez-Mó, 2014), and three members of this family (CD63, CD81 and CD9), held as classical exosome markers, were also detected in the current study (Table S3). The levels of CD63 were significantly

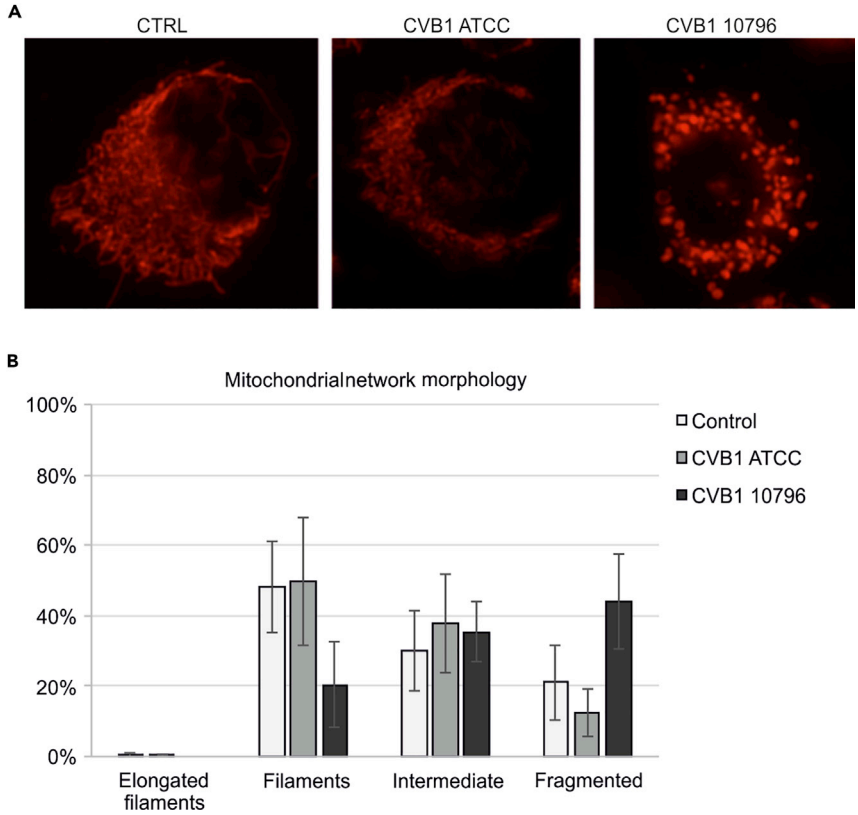


**Figure 4. Mitochondrial Networks in Non-infected PANC-1 Cells and Cells with Persistent CVB1 Infections**

Cell imaging analysis was carried out on three biological replicates of CVB1 ATCC persistent infection model and four biological replicates of CVB1 10796 persistent infection model and non-infected control cells.

(A) Mitochondrial network is visualized in living cells using MitoTracker staining. Representative examples of cells with persistent CVB1 ATCC and 10796 infection and non-infected control cells are shown.

(B) Cells were grouped into four different categories based on the morphology of their mitochondrial network. The data are presented as mean ± SD. Total numbers of cells used for the grouping: control *N* = 784, CVB1 ATCC *N* = 546, CVB1 10796 *N* = 709.

downregulated in the cell culture supernatants of the CVB1 ATCC model, whereas the secretion of another exosome marker, CD9, was significantly downregulated in cells persistently infected with CVB1 10796 strain. The persistent CVB1 infections did not change the secretion of CD81 (Figure 5A).

Based on SignalP analysis (Petersen et al., 2011), 371 differentially expressed proteins in the cell culture supernatants carry a signal peptide and are therefore likely to be secreted via the classical endoplasmic reticulum (ER)-Golgi pathway. Coxsackievirus proteins have previously been reported to inhibit protein trafficking through the Golgi (Cornell et al., 2006; de Jong et al., 2006), and in the current study the secretion of 225 and 218 proteins with predicted signal peptide was also downregulated in cells with persistent CVB1 ATCC and 10796 infection, respectively. Of those proteins 135 were commonly downregulated in the cell culture supernatants of CVB1 ATCC- and 10796-infected PANC-1 cells, whereas only five proteins with a predicted signal peptide were upregulated in the cell culture supernatants of both persistent infection models. One of these five upregulated proteins was macrophage colony stimulating factor 1 (CSF1), a cytokine with increased production reported in mouse heart tissues at the acute state of CVB3-induced myocarditis (Meyer et al., 2018).

In particular, persistent CVB1 infection was associated with clearly downregulated secretion of all five granin family members detected in the present study: chromogranin-B (also called secretogranin-1) (CHGB), secretogranin-2 (SCG2), secretogranin-3 (SCG3), neurosecretory protein VGF (VGF), and ProSAAS (PCSK1N) (Figures 5B and 5C). The granin family members have essential roles in the regulated secretory

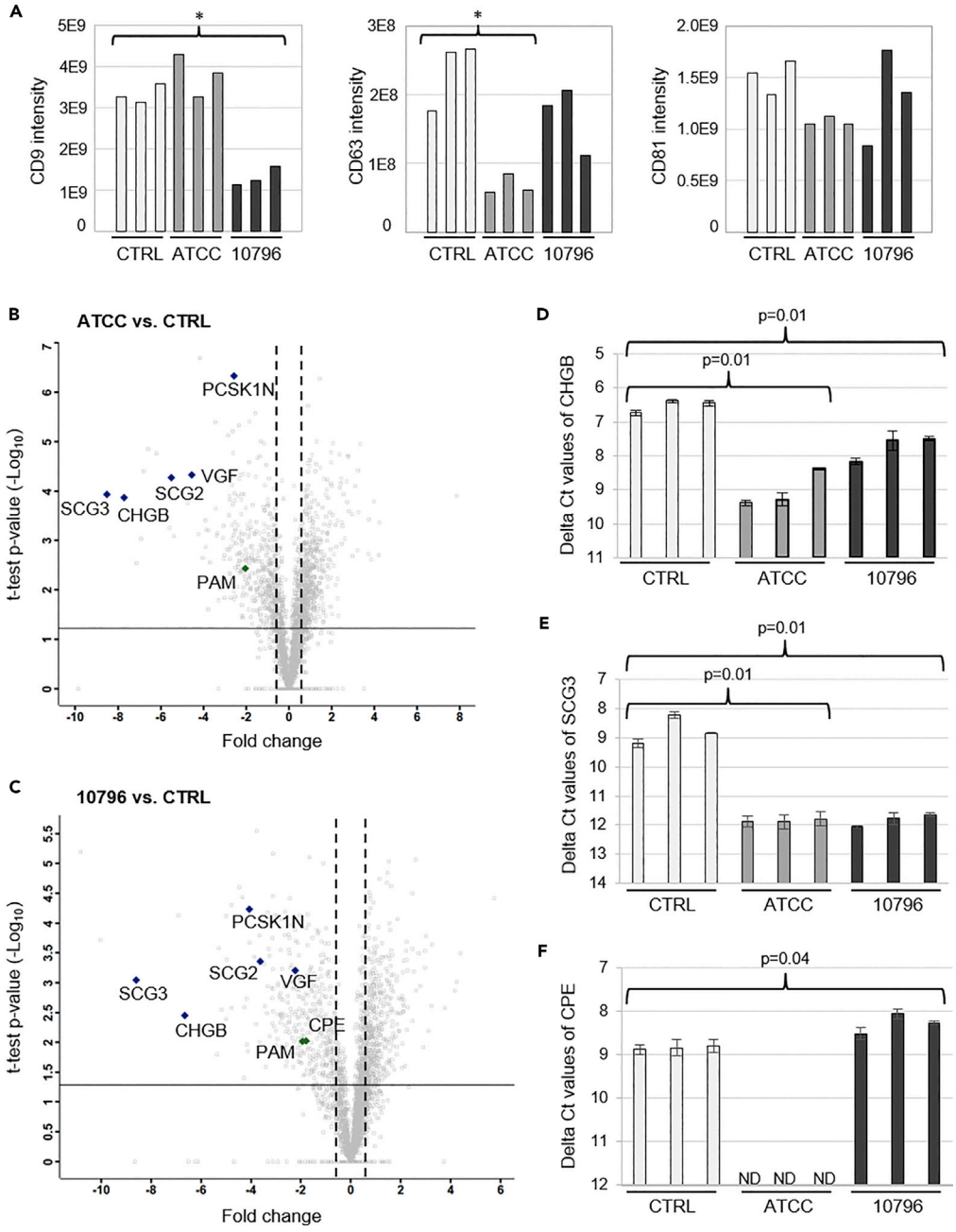


**Figure 5. Persistent CVB1 Infection Influences the Secretion of Several Proteins**

(A) Secretion of exosome marker proteins CD9, CD63, and CD81 from PANC-1 cells. For each sample, the median intensity of three technical replicates is shown. Statistically significant differences are marked with *.

(B and C) Persistent CVB1 ATCC (B) and 10796 (C) infection induced changes in the levels of extended granin family proteins, CPE and peptidylglycine α-amidating monooxygenase (PAM) in the cell culture supernatants.

(D–F) RT-qPCR analyses of CHGB (D), SCG3 (E), and CPE (F) in PANC-1 cells. The measurements were performed for the three biological replicates from each condition, and results are shown as Delta Ct ± SD. Primer sequences are presented in Table S7.

pathway, which is responsible of rapid on-demand secretion of hormones, growth factors, neurotransmitters, and other molecules. Proteins secreted through this pathway are directed from the *trans*-Golgi network to dense core granules, where they are stored at high concentrations until an extracellular signal stimulates their secretion. The granin family members present critical roles in the regulated secretory

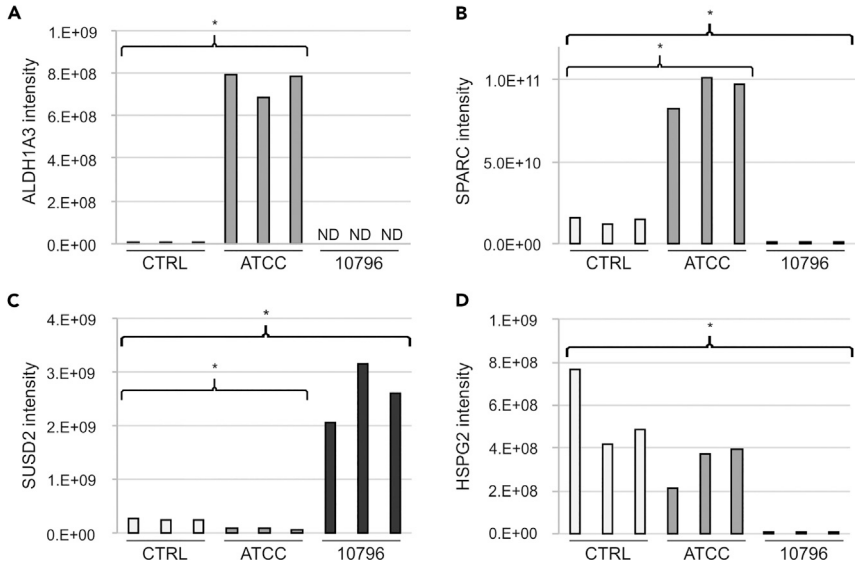


**Figure 6. Persistent CVB1 Infections Influence the Expression of Several Proteins Associated with Beta-Cell Differentiation, Growth, and Survival**

Persistent CVB1 infection induced changes in the expression levels of (A) ALDH1A3 (cell lysates), (B) SPARC (cell culture supernatants), (C) SUSD2 (cell lysates), and (D) HSPG2 (cell lysates). For each sample, median intensity of the three technical replicates is shown. Statistically significant differences are marked with *. ND, not detected.

pathway especially in granule biogenesis and protein sorting and also give rise to biologically active peptides (Huh et al., 2003; Hosaka et al., 2004; Courel et al., 2010; Bartolomucci et al., 2011). In addition to the granin family members, two well-known processing enzymes present in the regulated secretory pathway, peptidylglycine α-amidating monooxygenase (PAM) and carboxypeptidase E (CPE) (Eipper et al., 1993; Ji et al., 2017), were clearly downregulated or undetectable in the cell culture supernatants of the persistently CVB1-infected cells (Figures 5B and 5C). Further RT-qPCR analyses showed the downregulation of the granin family members CHGB and SCG3 already at transcriptional level, whereas the processing enzyme CPE remained undetectable at mRNA level in cells with persistent CVB1 ATCC infection but was significantly upregulated at mRNA level in cells with persistent CVB1 10796 infection (Figures 5D–5F). In summary, our results indicate that persistent CVB1 infections can interfere with protein secretion from the cells at multiple different levels.

## Proteins Associated with Pancreatic Beta-Cell Differentiation and Survival Are Strongly Affected by Persistent Coxsackievirus B1 Infection

Acute virus-like infection induces dedifferentiation in a human beta-cell line (Oshima et al., 2018). On the other hand, persistent CVB4 infection of PANC-1 cells downregulates the transcription factor PDX1, which is important for the formation of the endocrine pancreas (Sane et al., 2013). Interestingly, some of the proteins with the strongest infection-associated changes in the PANC-1 cells in the current study have also been linked with pancreatic beta-cell differentiation or survival. Furthermore, clear differences in the expression of a few of these proteins were observed between the two persistent infection models.

The most strongly upregulated protein in cells with persistent CVB1 ATCC infection was aldehyde dehydrogenase 1a3 (ALDH1A3), which has been used as a marker of dedifferentiated pancreatic beta-cells (Cinti et al., 2016; Kim-Muller et al., 2016). On the other hand, ALDH1A3 was not detected at all in cells with persistent CVB1 10796 infection, indicating its downregulation in this persistent infection model (Figure 6A). Matricellular protein SPARC is secreted by the cells of the endocrine and exocrine pancreas, and it can have a negative impact on beta-cell growth and survival (Ryall et al., 2014). It was the fourth most strongly upregulated protein in cells with persistent CVB1 ATCC infection, and its secretion from these cells was also significantly upregulated (Figure 6B). Similarly to ALDH1A3, SPARC was not detected in cells with persistent CVB1 10796 infection, and its secretion was strongly downregulated during persistent infection with CVB1 10796. Upregulation of the sushi domain-containing protein 2 (SUSD2) has been used to mark a particular stage in the maturation of endocrine pancreas during human fetal pancreatic differentiation

(Ramond et al., 2017). In the current study, SUSD2 was the third most strongly upregulated protein in cells persistently infected with CVB1 10796 strain, whereas its expression was significantly downregulated in the cells with persistent CVB1 ATCC infection (Figure 6C). Finally, heparan sulfate proteoglycan core protein (HSPG2) was the most strongly downregulated protein in cells with persistent CVB1 10796 infection, whereas it was not differentially expressed in cells with persistent CVB1 ATCC infection (Figure 6D). HSPG2 and laminin subunit alpha-5 (LAMA5), also strongly downregulated in cells with persistent CVB1 10796 infection, are components of human peri-islet basement membrane, which protects pancreatic islets from immune cell infiltration and thereby from beta-cell killing (Korpos et al., 2013; Otonkoski et al., 2008).

### Persistent Coxsackievirus B1 Infections Can Both Activate and Shut Down Host Antiviral Immune Responses

Acute CVB infection in human pancreatic islets induces strong type III interferon (IFN) responses (Lind et al., 2013; Ylipaasto et al., 2012). In the current study, interferon lambda-1 (IFNL1) secretion was observed from PANC-1 cells with persistent CVB1 ATCC infection. Interestingly, no IFNL1 was detected in the secretomes of cells persistently infected with CVB1 10796 or in the secretomes of non-infected control cells (Figure 7A). RT-qPCR analyses supported these findings, showing IFNL1 mRNA expression only during persistent CVB1 ATCC infection (Figures 7B and S1). Also in general, the activation of antiviral immune responses was clearly observed in persistent CVB1 ATCC infection model, whereas these responses were downregulated in persistent CVB1 10796 infection model when compared with non-infected PANC-1 cells. Based on IPA analysis, 14 of the 26 downstream targets of IFNL1 that were quantified in the cell lysates were significantly upregulated during persistent infection with ATCC strain of CVB1 (Figure 7C). In contrast, none of these proteins was upregulated in the CVB1 10796 persistent infection model. Of the IFNL1 downstream target proteins, 11 were significantly downregulated in the cells with persistent CVB1 10796 infection and additional nine IFNL1 downstream target proteins were undetectable in these cells, although they were detected in the non-infected PANC-1 cells (Figure 7D). The expression of a cytosolic viral RNA receptor interferon-induced helicase C domain-containing protein 1 (IFIH1) was studied further using *in situ* hybridization. The data from two different time points, the latter one 72 days before the proteomics sample collection, confirmed the high IFIH1 expression in samples from CVB1 ATCC persistent infection and low expression or absence of IFIH1 in the CVB1 10796 persistent infection model and the non-infected control cells (Figure 7E). Also, other proteins associated with antiviral immune responses were significantly upregulated in cells with persistent CVB1 ATCC infection, whereas downregulated or undetected in cells with persistent CVB1 10796 infection, including immunoproteasome component PSMB8, Endoplasmic reticulum aminopeptidase 2 (ERAP2) involved in peptide trimming, tapasin (TAPBP) involved in peptide loading on major histocompatibility complex class I, and human leukocyte antigen-C (HLA-C) (Table S2). Finally, persistent CVB1 ATCC infection also upregulated the secretion of several proteins involved in antiviral immune responses, including interleukin-18 (IL-18), and ubiquitin-like protein ISG15, whereas their secretion from cells with persistent CVB1 10796 infection was lower than that from the non-infected cells (Table S3).

## DISCUSSION

In the current study, two persistent CVB1 infection models were established in human PANC-1 cell line, and the infection-associated changes in the cells were characterized using proteomics approaches. Both intracellular proteome and secretome were profiled to understand the infection-induced changes in cell function and intercellular communication. To understand the range of responses that can be triggered by persistent CVB1 infections, the models were established using two CVB1 strains with clearly different abilities to induce innate immune responses based on our previous studies (immunogenic ATCC strain and less immunogenic 10796 strain) (Hamalainen et al., 2014). Although only a small proportion of the cells in both persistent infection models were virus-positive based on IHC staining of the viral VP1 protein, broad changes in protein expression and secretion were observed in both persistent infection models.

Carrier-state persistent infections are characterized by high titers of virus produced by a small number of infected cells (Alidjinou et al., 2017; Pinkert et al., 2011). Several changes observed in the current persistent CVB1 infection models support the presence of carrier-state persistence in the CVB1-infected PANC-1 cells. Studies on acute CVB infections have revealed multiple means by which CVBs modify the host cell functions for improved viral replication (Ilnytska et al., 2013; Albulescu et al., 2015; Lee et al., 2017). In the current study, several changes, which are likely beneficial for viral replication, were observed in both persistent infection models. Active replication of the virus was also confirmed in both persistent infection models by the detection of infective viral particles, viral VP1 protein, and viral genome as well as the

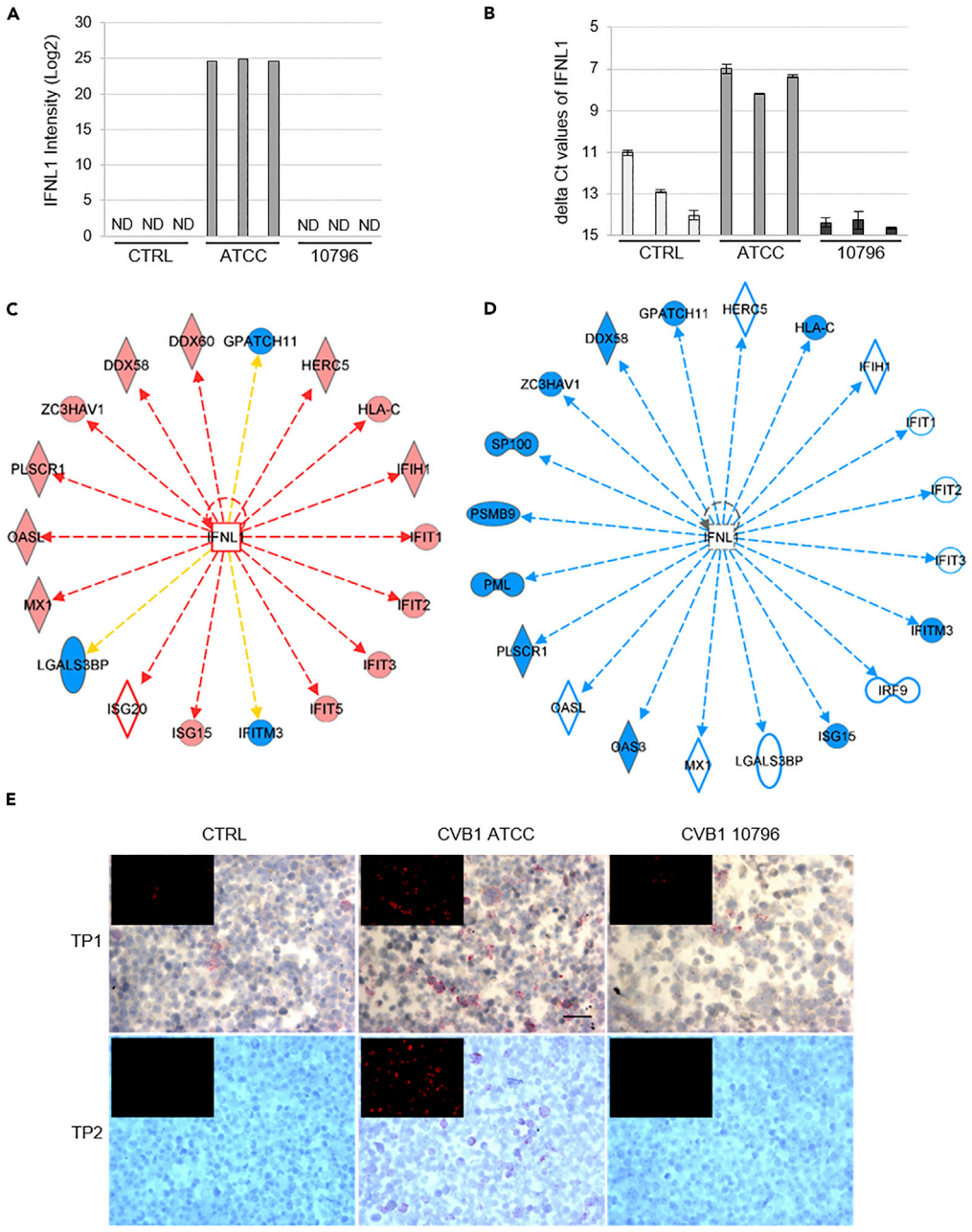


**Figure 7. Antiviral Immune Responses during Persistent CVB1 Infections**

(A) Changes in IFNL1 secretion from PANC-1 cells. For each sample, median intensity of three technical replicates is shown. ND, not detected.

(B) IFNL1 mRNA expression in PANC-1 cells. The measurements were performed for the three biological replicates from each condition. Primer sequences are presented in Table S7.

(C-D) Differentially expressed IFNL1 downstream target proteins in cells with persistent (C) CVB1 ATCC and (D) CVB1 10796 infection based on IPA analysis. Red, significantly upregulated; blue, significantly downregulated; white node with red lines, detected only in the cells with persistent CVB1 ATCC infection; white node with blue lines, not detected in the cells with persistent CVB1 10796 infection.

(E) IFIH1 expression in PANC-1 cells based on *in situ* hybridization. TP1, 102 days post-infection; TP2, 228 days post-infection. Scale bar, 50 μm. In each bright-field image, fluorescent channel from the bright-field image is condensed into corner.

detection of viral proteins in cell lysates and cell culture supernatants in the proteomic analyses. After viral replication, the infectious cycle of CVBs is usually completed via lytic release of mature virions from the infected cells, followed by the infection of "naive" cells via their CVB receptor CXADR (Bergelson et al., 1997). The lack of extensive cell lysis and the low number of virus-positive cells in carrier-state persistent infections can be partly explained by the downregulation of the CVB receptor CXADR observed in both persistent CVB1 infection models in the current study and in earlier models of carrier-state CVB persistency (Alidjinou et al., 2017; Pinkert et al., 2011). CVBs can also bind to another receptor DAF (CD55) on cell surface, but cannot undergo uncoating using that receptor (Bergelson and Coyne, 2013). Here, the expression of DAF was not detected in the cell lysates and was detected only in the cell culture supernatants of the non-infected PANC-1 cells. Furthermore, it is possible that the virus adapts to use other cellular receptors, as new receptors for enteroviruses are still being discovered (Zhao et al., 2019). Pathway analysis of the current proteomics data also revealed broader downregulation of proteins potentially involved in virus entry in both persistent CVB1 infection models, which could further limit the spreading of the virus. Previously it has been shown that CVBs may also spread directly from cell to cell via cellular protrusions (Paloheimo et al., 2011). Finally, microvesicles expressing autophagosome markers, in particular LC3, have recently been reported as a non-lytic means for the transmission of CVBs (Robinson et al., 2014; Sin et al., 2017). Downregulation of LC3 B in the cell culture supernatants of both persistent infection models (Table S3) could be associated with additional limitations in viral spreading via microvesicles during CVB1 persistency.

CVB proteins 2B, 2BC, and 3A have been shown to target the Golgi complex of the infected cell and to disrupt protein trafficking through it (Campanella et al., 2004; Cornell et al., 2006; de Jong et al., 2006; van Kuppeveld et al., 1997). Accordingly, acute CVB infections have been shown to modulate the secretory pathway of the infected cells (Cornell et al., 2006; de Jong et al., 2006), including pancreatic beta-cells (M.F.-T., unpublished data). CVB protein 2B can form pores in the ER and Golgi membranes resulting in $Ca^{2+}$ and $H^{+}$ release from these intracellular stores (van Kuppeveld et al., 1997; Campanella et al., 2004; de Jong et al., 2006). Acute infection of HeLa cells with CVB3 resulted in complete destruction of the Golgi complex, which was also observed after transfecting the cells with CVB3 3A protein alone (Cornell et al., 2006). In the current study, persistent CVB1 infections were associated with broad downregulation of proteins likely secreted via the classical secretory pathway in the cell culture supernatants of PANC-1 cells. In particular, proteins of the regulated secretory pathway were strongly downregulated in the secretomes of PANC-1 cells with persistent CVB1 infection. Maintenance of the $Ca^{2+}$ and pH homeostasis in the ER and Golgi is important for many of these proteins, including CPE and the granin family members. $Ca^{2+}$ and pH regulate the processing of pro-CPE and the activity of CPE, and $Ca^{2+}$ and pH-dependent aggregation of CPE and granins has been proposed to act as a sorting mechanism directing these proteins to the regulated secretory pathway (Chanat and Huttner, 1991; Ji et al., 2017; Song and Fricker, 1995). Interestingly, although CPE protein was significantly downregulated in the cell culture supernatants of the persistent CVB1 10796 infection model, significant upregulation of CPE mRNA was observed in the cells in this model, indicating infection-associated defects in the secretion of this protein. The possible infection-associated disruption of $Ca^{2+}$ and pH homeostasis in the ER and Golgi might have affected the sorting of CPE to the regulated secretory pathway, and/or the potential virus-induced destruction of the Golgi complex could have inhibited its trafficking through the regulated secretory pathway. Even if CPE was correctly addressed to the regulated secretory pathway, virus-induced alterations in pH and $Ca^{2+}$ levels are likely to influence its enzymatic activity. CPE is a crucial protein, for example, for insulin maturation, and reduced CPE activity has been associated with elevated levels of proinsulin and reduced levels of biologically active insulin in mouse models (Naggert et al., 1995).

ER stress is often induced by viral infections, including CVB infections (Colli et al., 2019; Zhang et al., 2010). The type of these responses can vary depending on the cell type and the virus. The expression of one ER stress protein, ER chaperone BiP (HSPA5) detected also in the current study, was shown to be induced by acute CVB3 infection of HeLa and HL-1 cells (Zhang et al., 2010), whereas CVB5 infection of human beta-cell line EndoC-βH1 did not change the expression of this protein (Colli et al., 2019). Instead, partial ER stress via IRE1α phosphorylation was shown to be induced by CVB5 infection of EndoC-βH1 cells (Colli et al., 2019). In the current study, the expression of HSPA5 was significantly downregulated during persistent CVB1 10796 infection and slightly reduced during persistent CVB1 ATCC infection. Whether signs of partial ER stress can be induced during persistent CVB infection remains to be studied.

In addition to the features common for the two persistent CVB1 infection models, several differences were detected between these models. These differences could be associated with the distinct properties of the ATCC and 10796 virus strains, random mutations accumulated in these viruses during persistency, or with different kinetics of the infection-induced responses between the two persistent infection models.

The kinetics and magnitude of antiviral immune responses triggered by acute enterovirus infections differ between distinct virus strains (Anagandula et al., 2014; Hamalainen et al., 2014; Ylipaasto et al., 2012). Differences in the immunogenic properties of these viruses could also influence their ability to persist in infected cells or tissues. Based on our earlier studies, acute infection of human peripheral blood mononuclear cells (PBMCs) and dendritic cells with CVB1 ATCC strain clearly triggers a stronger upregulation of antiviral immune responses than a similar infection with the CVB1 10796 strain (Hamalainen et al., 2014). Furthermore, the infection of human pancreatic islets with CVB1 10796 strain only results in moderate cytopathic effects (Anagandula et al., 2014). Still, an acute infection with the less immunogenic CVB1 10796 strain induces antiviral immune responses both in human pancreatic islets (Anagandula et al., 2014) and in human PBMCs (Hamalainen et al., 2014; Lietzen et al., 2018). In the current study, persistent infection with the ATCC strain of CVB1 was associated with IFNL1 secretion, upregulation of several IFNL1 downstream target proteins, and upregulation of multiple other proteins involved in antiviral immune responses. These changes are in line with the antiviral immune responses triggered by different CVBs in, for example, human pancreatic islets during acute infection (Ylipaasto et al., 2005, 2012; Lind et al., 2013, 2016; Nyalwidhe et al., 2017). In addition, immunofluorescence analyses of pancreatic tissue samples from organ donors with low-grade enterovirus infection and T1D have shown the presence of antiviral EIF2AK2 in cells positive for enterovirus VP1 protein (Richardson et al., 2009, 2013). Interestingly, in this study persistent CVB1 10796 infection resulted in an apparent shutdown of these host antiviral immune responses as indicated by the downregulation of numerous antiviral immune response proteins when compared with non-infected controls. Furthermore, downregulated secretion of immune response proteins, including pro-inflammatory cytokine IL-18, IFNL1, and ISG15, as observed in persistent 10796 infection, would make the infected cells less visible for the immune system, likely delaying their clearance.

The ability of a virus to circumvent host antiviral responses can provide important advantages, reducing infection-induced stress in the cells and thereby allowing prolonged infection. In the current study, viral proteins were more abundant in the cells and in the cell culture supernatants of persistent CVB1 10796 infection model when compared with the persistent CVB1 ATCC infection model, which could influence more efficient blocking of host antiviral immune responses during persistent CVB1 10796 infection. Also in an earlier study monitoring the growth kinetics of CVB1 strains in HeLa cells within a 48-h time frame, CVB1 10796 was shown to replicate faster and produce more virus progeny than CVB1 ATCC strain (Hamalainen et al., 2014).

Mitochondrial antiviral-signaling protein (MAVS) is a central protein in host antiviral immune responses, and signaling via MAVS, residing on mitochondrial or peroxisomal membranes, can induce type III IFN responses (Bender et al., 2015; Odendall et al., 2014). CVBs can use different strategies to suppress MAVS-mediated host antiviral immune responses, and clearly reduced type I (Mukherjee et al., 2011; Feng et al., 2014; Lind et al., 2016) and type III IFN responses (Lind et al., 2016) after acute CVB infections have been observed in a few studies. CVB protease 2A can cleave MAVS resulting in suppressed type I and type III IFN responses (Feng et al., 2014; Lind et al., 2016). According to our data MAVS was significantly downregulated in the cells with persistent CVB1 10796 infection, whereas its expression in the CVB1 ATCC model was only slightly, but not significantly, reduced when compared with the non-infected control cells (Table S2). The clear downregulation of MAVS in the cells with persistent CVB1 10796 infection could be associated with, for example, higher expression of viral proteins in this model or with more efficient targeting of MAVS by the CVB1 10796 protease 2A. Mitochondrial network fragmentation can also downregulate MAVS-mediated antiviral signaling (Castanier et al., 2010). For example, cytomegalovirus inhibits MAVS-mediated antiviral signaling by promoting fragmentation of the mitochondrial network (McCormick et al., 2003), Dengue virus NS2B3 protease can attenuate cellular antiviral immunity by cleaving the mitochondrial fusion proteins MFN1 and MFN2 (Yu et al., 2015), and hepatitis C virus can induce mitochondrial fragmentation by stimulating the dynamin-related protein 1 (DRP1) involved in mitochondrial fission (Kim et al., 2014). Fragmented mitochondrial network has also been observed in murine cardiomyocytes during acute CVB3 infection (Sin et al., 2017), and in the current study over 40% of the cells in CVB1 10796

persistent infection model had fragmented mitochondrial network. Based on these results, persistent infection with 10796 strain of CVB1 is likely attenuating MAVS-mediated antiviral signaling more efficiently than persistent infection with the ATCC strain of CVB1. However, other regulatory mechanisms are also probably required to reach the broad downregulation of antiviral immune responses when compared with the non-infected control cells.

Some of the strongest changes observed in the current persistent infection models involved proteins that also have a role in pancreatic beta-cell function, differentiation, growth, and survival. Low-grade enterovirus infections in human pancreatic islets have been associated with T1D in multiple studies (Yoon et al., 1979; Richardson et al., 2009, 2013; Krogvold et al., 2015). Persistent CVB4 infection in PANC-1 cells has been shown to result in the downregulation of PDX1, a transcription factor important for the development and function of pancreatic beta-cells (Sane et al., 2013), and in the dysregulation of a set of microRNAs with many of them potentially targeting T1D risk genes (Engelmann et al., 2017). In this study, both persistent CVB1 infections resulted in strong downregulation of the key players of the regulated secretory pathway, which in beta-cells is also responsible for insulin processing and secretion. This is in line with an earlier study showing lower levels of insulin in beta-cells positive for the enterovirus VP1 protein in pancreatic tissue samples from organ donors with T1D (Richardson et al., 2013). Strong opposite changes induced by the two persistent CVB1 infection models were observed in the expression of three proteins associated with pancreatic beta-cell differentiation, growth, and survival: ALDH1A3 (Cinti et al., 2016; Kim-Muller et al., 2016), SPARC (Ryall et al., 2014) and SUSD2 (Ramond et al., 2017). In addition, persistent CVB1 10796 infection of PANC-1 cells resulted in significantly reduced expression of two human peri-islet basement membrane proteins, HSPG2 and LAMA5 (Korpos et al., 2013; Otonkoski et al., 2008), and also the secretion of HSPG2 was strongly downregulated in this persistent infection model. The reduced expression and secretion of peri-islet basement membrane components could shift the balance between membrane destruction and repair, making pancreatic islets more susceptible to leukocyte infiltration and beta-cell killing during enterovirus infection. Finally, increased secretion of CSF1 was observed in both persistent infection models. CSF1 and its receptor (CSF1R) play essential roles in the development of monocytes and in macrophage proliferation (Chitu and Stanley, 2006). Increased expression of CSF1 has been reported in patients with myocarditis, and in a mouse model of CVB3-induced myocarditis suppression of the CSF1 was shown to reduce the inflammatory outcome and decrease the levels of infiltrating leukocytes (Meyer et al., 2018). Moreover, depletion of pancreatic islet-resident macrophages by monoclonal autoantibody against CSF1R reduced the development of autoimmune diabetes in NOD mice, indicating the importance of these cells in the disease pathogenesis (Carrero et al., 2017).

Very recently, a study by Nekoua et al. described the establishment of persistent CVB4 infection in a beta-cell-like cell line 1.1B4 and showed that the cells with persistent CVB4 infection are targets of natural killer cell-mediated lysis (Nekoua et al., 2019). Still, the expression of insulin mRNA was not detected in these cells. Future studies are needed to understand the benefits of this persistent infection model in studying the potential outcomes of persistent CVB infections in human pancreas.

The current study provides a broad characterization of the changes induced by persistent CVB1 infection in a human pancreatic ductal-like cell line. The parallel analysis of two distinct persistent infection models utilizing CVB1 strains with different immunogenic properties is an important step towards understanding the potential heterogeneity of the virus-cell interactions, which regulate the development of viral persistency and its effects on the cell. Some of the changes observed in the current study are similar to the responses triggered by acute enterovirus infections in human pancreatic islets, but importantly, our results also show strong contrasting changes between the two persistent infection models not reported with acute enterovirus infections. Further studies on persistent CVB infections are required to better understand the origins of these differences. Finally, in the light of recent, but still very limited, data on the presence of CVBs also outside pancreatic islets (Busse et al., 2017), we speculate that pancreatic ductal cells could also act as sites for enterovirus persistence enabling from time to time spreading of the virus into the beta-cells. Larger studies evaluating systematically the presence of these viruses in the endocrine and exocrine pancreas are needed to further test this hypothesis. Overall, the current study covers novel information on persistent CVB infection-induced changes in protein expression and secretion in a human pancreatic ductal-like cell line and thereby provides new ideas for studying the pathogenic mechanisms of persistent enterovirus infections in human pancreas tissue samples.

### Limitations of the Study

Persistent CBV infection models established in human pancreatic cell lines are valuable tools to study the potential outcomes of chronic CVB infections in human pancreas. One of the limitations of the current study is the use of PANC-1 cell line instead of an insulin-producing human beta-cell line as a model system. Despite the increasing amounts of evidence on connections between enterovirus infections and the development of T1D, persistent CVB infection models have, to our knowledge, not yet been published in an insulin-producing beta-cell line. Such studies would bring important insights into host-virus interplay during prolonged CVB infection of pancreatic beta-cells. On the other hand, further mechanistic and functional studies utilizing the existing persistent infection models would already bring deeper understanding on the infection-induced responses observed in the current study. Finally, additional studies are needed for comprehensive mapping of mutations in viral genomes acquired during persistency, and to understand whether certain changes in viral genome are required for the formation of carrier-state persistent infections.

## METHODS

All methods can be found in the accompanying Transparent Methods supplemental file.

## DATA AND CODE AVAILABILITY

The raw mass spectrometry data have been deposited to the ProteomeXchange Consortium (http://proteomecentral.proteomexchange.org) via the PRIDE partner repository (Vizcaíno et al., 2012) with the dataset identifiers PXD012153 and PXD012154.

## SUPPLEMENTAL INFORMATION

Supplemental Information can be found online at https://doi.org/10.1016/j.isci.2019.07.040.

## ACKNOWLEDGMENTS

We wish to thank Professor Didier Hober (University of Lille, Lille, France) for his valuable help with the persistent infection models. Eini Eskola, Anne Karjalainen, Mervi Kekäläinen, Tanja Kuusela, Maria Ovaskainen, Eveliina Palomäki, and Eeva Tolvanen (Faculty of Medicine and Health Technology, Tampere University) are acknowledged for their technical support. University of Turku Virology laboratory led by Professor Ilkka Julkunen is acknowledged for their help and facilities for proteomics sample preparation. Sarita Heinonen (Turku Bioscience Center, University of Turku) is acknowledged for the technical assistance. The LC-MS/MS analyses presented in this work were performed at the Proteomics Core Facility of the Turku Bioscience Center that belongs to Biocenter Finland infrastructure network. The microscopy experiments were performed at Tampere Imaging Facility, BioMediTech, Faculty of Medicine and Health Technology, Tampere University.

This work was financially supported by the Academy of Finland decisions no. 287423, 288671, 292482, 292335, 294337, 319280, and 314444; Sigrid Jusélius Foundation; Juvenile Diabetes Research Foundation Ltd (JDRF); Finnish Diabetes Research Foundation; Turku University Foundation; Maud Kuistila Foundation; and Reino Lahtikari Foundation. The project has also received funding from the Innovative Medicines Initiative 2 Joint Undertaking under grant agreement No 115797 (INNODIA). This Joint Undertaking receives support from the Union's Horizon 2020 research and innovation program and "EFPIA," "JDRF," and "The Leona M. and Harry B. Helmsley Charitable Trust. Studies at Karolinska Institutet were supported by grants to M.F.-T from Karolinska Institutet including the Strategic Research Program in Diabetes, the Swedish Research Council, and a grant from the Swedish Child Diabetes Foundation.

## AUTHOR CONTRIBUTIONS

N.L. and K.H. designed the proteomics experiments, prepared the proteomics samples, performed the mass spectrometry experiments, and processed and analyzed the proteomics data. A.H. and A.-B.S.-K. established the persistent infection model, and A.H. cultured the cells and provided the samples. T.B., M.A.M., and M.F.-T. performed the Taqman analyses. J.E.L. was responsible for the IHC stainings and analyzed the samples. A.H. and A.-B.S.-K. performed the mitochondrial imaging experiments. E.D. helped with the mitochondrial imaging experiments. S.O. performed the virus RT-PCR analyses. N.L., K.H., and T.B. performed the western blot experiments. A.H. performed the cell viability analyses. N.L., K.H., and A.H. wrote the paper with the help of T.B. A.-B.S.-K. critically revised the manuscript. R.L. and H.H. initiated

and supervised the study and critically revised the manuscript. All authors have contributed to the final version of the manuscript.

## DECLARATION OF INTERESTS

H.H. is a shareholder and chairman of the board of Vactech Ltd (http://www.vactech.fi/en/), which develops vaccines against picornaviruses.

Received: April 4, 2019
Revised: July 8, 2019
Accepted: July 25, 2019
Published: September 27, 2019

## REFERENCES

Albulescu, L., Wubbolts, R., van Kuppeveld, F.J., and Strating, J.R. (2015). Cholesterol shuttling is important for RNA replication of coxsackievirus B3 and encephalomyocarditis virus. Cell. Microbiol. *17*, 1144–1156.

Alidjinou, E.K., Engelmann, I., Bossu, J., Villenet, C., Figeac, M., Romond, M.B., Sane, F., and Hober, D. (2017). Persistence of Coxsackievirus B4 in pancreatic ductal-like cells results in cellular and viral changes. Virulence *8*, 1229–1244.

Anagandula, M., Richardson, S.J., Oberste, M.S., Sioofy-Khojine, A.-B., Hyöty, H., Morgan, N.G., Korsgren, O., and Frisk, G. (2014). Infection of human islets of langerhans with two strains of coxsackie B virus serotype 1: Assessment of virus replication, degree of cell death and induction of genes involved in the innate immunity pathway. J. Med. Virol. *86*, 1402–1411.

Andreu, Z., and Yáñez-Mó, M. (2014). Tetraspanins in extracellular vesicle formation and function. Front. Immunol. *5*, 442.

Bartolomucci, A., Possenti, R., Mahata, S.K., Fischer-Colbrie, R., Loh, Y.P., and Salton, S.R.J. (2011). The extended granin family: structure, function, and biomedical implications. Endocr. Rev. *32*, 755–797.

Belov, G.A., Evstafieva, A.G., Rubtsov, Y.P., Mikitas, O.V., Vartapetian, A.B., and Agol, V.I. (2000). Early alteration of nucleocytoplasmic traffic induced by some RNA viruses. Virology *275*, 244–248.

Bender, S., Reuter, A., Eberle, F., Einhorn, E., Binder, M., and Bartenschlager, R. (2015). Activation of type I and III interferon response by mitochondrial and peroxisomal MAVS and inhibition by hepatitis C virus. PLoS Pathog. *11*, e1005264.

Bergelson, J.M., Cunningham, J.A., Droguett, G., Kurt-Jones, E.A., Krithivas, A., Hong, J.S., Horwitz, M.S., Crowell, R.L., and Finberg, R.W. (1997). Isolation of a common receptor for Coxsackie B viruses and adenoviruses 2 and 5. Science *275*, 1320–1323.

Bergelson, J.M., and Coyne, C.B. (2013). Picornavirus entry. In Viral Entry into Host Cells. Advances in Experimental Medicine and Biology, *790*, S. Pöhlmann and G. Simmons, eds., Viral Entry into Host Cells. Advances in Experimental Medicine and Biology (Springer), pp. 24–41.

Borman, A.M., Kirchweger, R., Ziegler, E., Rhoads, R.E., Skern, T., and Kean, K.M. (1997). eIF4G and its proteolytic cleavage products: effect on initiation of protein synthesis from capped, uncapped, and IRES-containing mRNAs. RNA *3*, 186–196.

Busse, N., Paroni, F., Richardson, S.J., Laiho, J.E., Oikarinen, M., Frisk, G., Hyöty, H., de Koning, E., Morgan, N.G., and Maedler, K. (2017). Detection and localization of viral infection in the pancreas of patients with type 1 diabetes using short fluorescently-labelled oligonucleotide probes. Oncotarget *8*, 12620–12636.

Campanella, M., de Jong, A.S., Lanke, K.W.H., Melchers, W.J.G., Willems, P.H.G.M., Pinton, P., Rizzuto, R., and van Kuppeveld, F.J.M. (2004). The coxsackievirus 2B protein suppresses apoptotic host cell responses by manipulating intracellular Ca2+ homeostasis. J. Biol. Chem. *279*, 18440–18450.

Carrero, J.A., McCarthy, D.P., Ferris, S.T., Wan, X., Hu, H., Zinselmeyer, B.H., Vomund, A.N., and Unanue, E.R. (2017). Resident macrophages of pancreatic islets have a seminal role in the initiation of autoimmune diabetes of NOD mice. Proc. Natl. Acad. Sci. U S A *114*, E10418–E10427.

Castanier, C., Garcin, D., Vazquez, A., and Arnoult, D. (2010). Mitochondrial dynamics regulate the RIG-I-like receptor antiviral pathway. EMBO Rep. *11*, 133–138.

Chanat, E., and Huttner, W.B. (1991). Milieu-induced, selective aggregation of regulated secretory proteins in the trans-Golgi network. J. Cell Biol. *115*, 1505–1519.

Chapman, N.M., and Kim, K.S. (2008). Persistent coxsackievirus infection: enterovirus persistence in chronic myocarditis and dilated cardiomyopathy. Curr. Top. Microbiol. Immunol. *323*, 275–292.

Chehadeh, W., Kerr-Conte, J., Pattou, F., Alm, G., Lefebvre, J., Wattré, P., and Hober, D. (2000). Persistent infection of human pancreatic islets by coxsackievirus B is associated with alpha interferon synthesis in beta cells. J. Virol. *74*, 10153–10164.

Chitu, V., and Stanley, E.R. (2006). Colony-stimulating factor-1 in immunity and inflammation. Curr. Opin. Immunol. *18*, 39–48.

Cinti, F., Bouchi, R., Kim-Muller, J.Y., Ohmura, Y., Sandoval, P.R., Masini, M., Marselli, L., Suleiman, M., Ratner, L.E., Marchetti, P., et al. (2016). Evidence of β-cell dedifferentiation in human type 2 diabetes. J. Clin. Endocrinol. Metab. *101*, 1044–1054.

Colli, M.L., Paula, F.M., Marselli, L., Marchetti, P., Roivainen, M., Eizirik, D.L., and Op de beeck, A. (2019). Coxsackievirus B tailors the unfolded protein response to favour viral amplification in pancreatic β cells. J. Innate Immun. *11*, 375–390.

Cornell, C.T., Kiosses, W.B., Harkins, S., and Whitton, J.L. (2006). Inhibition of protein trafficking by coxsackievirus B3: multiple viral proteins target a single organelle. J. Virol. *80*, 6637–6647.

Courel, M., Soler-Jover, A., Rodriguez-Flores, J.L., Mahata, S.K., Elias, S., Montero-Hadjadje, M., Anouar, Y., Giuly, R.J., O'Connor, D.T., and Taupenot, L. (2010). Pro-hormone secretogranin II regulates dense core secretory granule biogenesis in catecholaminergic cells. J. Biol. Chem. *285*, 10030–10043.

Eipper, B.A., Milgram, S.L., Husten, E.J., Yun, H.Y., and Mains, R.E. (1993). Peptidylglycine alpha-amidating monooxygenase: a multifunctional protein with catalytic, processing, and routing domains. Protein Sci. A Publ. Protein Soc. *2*, 489–497.

Engelmann, I., Alidjinou, E.K., Bertin, A., Bossu, J., Villenet, C., Figeac, M., Sane, F., and Hober, D. (2017). Persistent coxsackievirus B4 infection induces microRNA dysregulation in human pancreatic cells. Cell. Mol. Life Sci. *74*, 3851–3861.

Feng, Q., Langereis, M.A., Lork, M., Nguyen, M., Hato, S.V., Lanke, K., Emdad, L., Bhoopathi, P., Fisher, P.B., Lloyd, R.E., et al. (2014). Enterovirus 2Apro targets MDA5 and MAVS in infected cells. J. Virol. *88*, 3369–3378.

Frisk, G. (2001). Mechanisms of chronic enteroviral persistence in tissue. Curr. Opin. Infect. Dis. *14*, 251–256.

Gustin, K.E., and Sarnow, P. (2001). Effects of poliovirus infection on nucleo-cytoplasmic trafficking and nuclear pore complex composition. EMBO J. *20*, 240–249.

Hamalainen, S., Nurminen, N., Ahlfors, H., Oikarinen, S., Sioofy-Khojine, A.B., Frisk, G., Oberste, M.S., Lahesmaa, R., Pesu, M., and Hyoty, H. (2014). Coxsackievirus B1 reveals strain specific differences in plasmacytoid dendritic cell

mediated immunogenicity. J. Med. Virol. *86*, 1412–1420.

Hosaka, M., Suda, M., Sakai, Y., Izumi, T., Watanabe, T., and Takeuchi, T. (2004). Secretogranin III binds to cholesterol in the secretory granule membrane as an adapter for chromogranin A. J. Biol. Chem. *279*, 3627–3634.

Huh, Y.H., Jeon, S.H., and Yoo, S.H. (2003). Chromogranin B-induced secretory granule biogenesis: comparison with the similar role of chromogranin A. J. Biol. Chem. *278*, 40581–40589.

Hyoty, H. (2016). Viruses in type 1 diabetes. Pediatr. Diabetes *17* (*Suppl 2*), 56–64.

Ifie, E., Russell, M.A., Dhayal, S., Leete, P., Sebastiani, G., Nigi, L., Dotta, F., Marjomäki, V., Eizirik, D.L., Morgan, N.G., et al. (2018). Unexpected subcellular distribution of a specific isoform of the Coxsackie and adenovirus receptor, CAR-SIV, in human pancreatic beta cells. Diabetologia *61*, 2344–2355.

Ilnytska, O., Santiana, M., Hsu, N.Y., Du, W.L., Chen, Y.H., Viktorova, E.G., Belov, G., Brinker, A., Storch, J., Moore, C., et al. (2013). Enteroviruses harness the cellular endocytic machinery to remodel the host cell cholesterol landscape for effective viral replication. Cell Host Microbe *14*, 281–293.

Ji, L., Wu, H.-T., Qin, X.-Y., and Lan, R. (2017). Dissecting carboxypeptidase E: properties, functions and pathophysiological roles in disease. Endocr. Connect. *6*, R18–R38.

de Jong, A.S., Visch, H.-J., de Mattia, F., van Dommelen, M.M., Swarts, H.G., Luyten, T., Callewaert, G., Melchers, W.J., Willems, P.H., and van Kuppeveld, F.J. (2006). The coxsackievirus 2B protein increases efflux of ions from the endoplasmic reticulum and Golgi, thereby inhibiting protein trafficking through the Golgi. J. Biol. Chem. *281*, 14144–14150.

Kim-Muller, J.Y., Fan, J., Kim, Y.J.R., Lee, S.-A., Ishida, E., Blaner, W.S., and Accili, D. (2016). Aldehyde dehydrogenase 1a3 defines a subset of failing pancreatic β cells in diabetic mice. Nat. Commun. *7*, 12631.

Kim, K.S., Chapman, N.M., and Tracy, S. (2008). Replication of coxsackievirus B3 in primary cell cultures generates novel viral genome deletions. J. Virol. *82*, 2033–2037.

Kim, S.-J., Syed, G.H., Khan, M., Chiu, W.-W., Sohail, M.A., Gish, R.G., and Siddiqui, A. (2014). Hepatitis C virus triggers mitochondrial fission and attenuates apoptosis to promote viral persistence. Proc. Natl. Acad. Sci. U S A *111*, 6413–6418.

Knockenhauer, K.E., and Schwartz, T.U. (2016). The nuclear pore complex as a flexible and dynamic gate. Cell *164*, 1162–1171.

Korpos, É., Kadri, N., Kappelhoff, R., Wegner, J., Overall, C.M., Weber, E., Holmberg, D., Cardell, S., and Sorokin, L. (2013). The peri-islet basement membrane, a barrier to infiltrating leukocytes in type 1 diabetes in mouse and human. Diabetes *62*, 531–542.

Krogvold, L., Edwin, B., Buanes, T., Frisk, G., Skog, O., Anagandula, M., Korsgren, O., Undlien, D., Eike, M.C., Richardson, S.J., et al. (2015). Detection of a low-grade enteroviral infection in the islets of langerhans of living patients newly diagnosed with type 1 diabetes. Diabetes *64*, 1682–1687.

van Kuppeveld, F.J., Hoenderop, J.G., Smeets, R.L., Willems, P.H., Dijkman, H.B., Galama, J.M., and Melchers, W.J. (1997). Coxsackievirus protein 2B modifies endoplasmic reticulum membrane and plasma membrane permeability and facilitates virus release. EMBO J. *16*, 3519–3532.

Laitinen, O.H., Honkanen, H., Pakkanen, O., Oikarinen, S., Hankaniemi, M.M., Huhtala, H., Ruokoranta, T., Lecouturier, V., Andre, P., Harju, R., et al. (2014). Coxsackievirus B1 is associated with induction of beta-cell autoimmunity that portends type 1 diabetes. Diabetes *63*, 446–455.

Laitinen, O.H., Svedin, E., Kapell, S., Nurminen, A., Hytönen, V.P., and Flodström-Tullberg, M. (2016). Enteroviral proteases: structure, host interactions and pathogenicity. Rev. Med. Virol. *26*, 251–267.

Lee, K.-M., Chen, C.-J., and Shih, S.-R. (2017). Regulation mechanisms of viral IRES-driven translation. Trends Microbiol. *25*, 546–561.

Lietzen, N., An, L.T.T., Jaakkola, M.K., Kallionpää, H., Oikarinen, S., Mykkänen, J., Knip, M., Veijola, R., Ilonen, J., Toppari, J., et al. (2018). Enterovirus-associated changes in blood transcriptomic profiles of children with genetic susceptibility to type 1 diabetes. Diabetologia *61*, 381–388.

Lind, K., Richardson, S.J., Leete, P., Morgan, N.G., Korsgren, O., and Flodström-Tullberg, M. (2013). Induction of an antiviral state and attenuated coxsackievirus replication in type III interferon-treated primary human pancreatic islets. J. Virol. *87*, 7646–7654.

Lind, K., Svedin, E., Domsgen, E., Kapell, S., Laitinen, O.H., Moll, M., and Flodström-Tullberg, M. (2016). Coxsackievirus counters the host innate immune response by blocking type III interferon expression. J. Gen. Virol. *97*, 1368–1380.

Massilamany, C., Gangaplara, A., and Reddy, J. (2014). Intricacies of cardiac damage in coxsackievirus B3 infection: implications for therapy. Int. J. Cardiol. *177*, 330–339.

McCormick, A.L., Smith, V.L., Chow, D., and Mocarski, E.S. (2003). Disruption of mitochondrial networks by the human cytomegalovirus UL37 gene product viral mitochondrion-localized inhibitor of apoptosis. J. Virol. *77*, 631–641.

Meyer, I.S., Goetzke, C.C., Kespohl, M., Sauter, M., Heuser, A., Eckstein, V., Vornlocher, H.-P., Anderson, D.G., Haas, J., Meder, B., et al. (2018). Silencing the CSF-1 axis using nanoparticle encapsulated sirna mitigates viral and autoimmune myocarditis. Front. Immunol. *9*, 2303.

Mukherjee, A., Morosky, S.A., Delorme-Axford, E., Dybdahl-Sissoko, N., Oberste, M.S., Wang, T., and Coyne, C.B. (2011). The coxsackievirus B 3C protease cleaves MAVS and TRIF to attenuate host type I interferon and apoptotic signaling. PLoS Pathog. *7*, e1001311.

Naggert, J.K., Fricker, L.D., Varlamov, O., Nishina, P.M., Rouille, Y., Steiner, D.F., Carroll, R.J., Paigen, B.J., and Leiter, E.H. (1995). Hyperproinsulinaemia in obese fat/fat mice associated with a carboxypeptidase E mutation which reduces enzyme activity. Nat. Genet. *10*, 135–142.

Nekoua, M.P., Bertin, A., Sane, F., Alidjinou, E.K., Lobert, D., Trauet, J., Hober, C., Engelmann, I., Moutairou, K., Yessoufou, A., et al. (2019). Pancreatic beta cells persistently infected with coxsackievirus B4 are targets of NK cell-mediated cytolytic activity. Cell. Mol. Life Sci., In press. https://doi.org/10.1007/s00018-019-03168-4.

Nishtala, K., Phong, T.Q., Steil, L., Sauter, M., Salazar, M.G., Kandolf, R., Kroemer, H.K., Felix, S.B., Völker, U., Klingel, K., et al. (2011). Virus-induced dilated cardiomyopathy is characterized by increased levels of fibrotic extracellular matrix proteins and reduced amounts of energy-producing enzymes. Proteomics *11*, 4310–4320.

Nurminen, N., Oikarinen, S., and Hyoty, H. (2012). Virus infections as potential targets of preventive treatments for type 1 diabetes. Rev. Diabet. Stud. *9*, 260–271.

Nyalwidhe, J.O., Gallagher, G.R., Glenn, L.M., Morris, M.A., Vangala, P., Jurczyk, A., Bortell, R., Harlan, D.M., Wang, J.P., and Nadler, J.L. (2017). Coxsackievirus-induced proteomic alterations in primary human islets provide insights for the etiology of diabetes. J. Endocr. Soc. *1*, 1272–1286.

Odendall, C., Dixit, E., Stavru, F., Bierne, H., Franz, K.M., Durbin, A.F., Boulant, S., Gehrke, L., Cossart, P., and Kagan, J.C. (2014). Diverse intracellular pathogens activate type III interferon expression from peroxisomes. Nat. Immunol. *15*, 717–726.

Oikarinen, S., Tauriainen, S., Hober, D., Lucas, B., Vazeou, A., Sioofy-Khojine, A., Bozas, E., Muir, P., Honkanen, H., Ilonen, J., et al. (2014). Virus antibody survey in different European populations indicates risk association between coxsackievirus B1 and type 1 diabetes. Diabetes *63*, 655–662.

Oshima, M., Knoch, K.-P., Diedisheim, M., Petzold, A., Cattan, P., Bugliani, M., Marchetti, P., Choudhary, P., Huang, G.-C., Bornstein, S.R., et al. (2018). Virus-like infection induces human β cell dedifferentiation. JCI Insight *3*, 97732.

Otonkoski, T., Banerjee, M., Korsgren, O., Thornell, L.-E., and Virtanen, I. (2008). Unique basement membrane structure of human pancreatic islets: implications for beta-cell growth and differentiation. Diabetes Obes. Metab. *10* (*Suppl 4*), 119–127.

Paloheimo, O., Ihalainen, T.O., Tauriainen, S., Välilehto, O., Kirjavainen, S., Niskanen, E.A., Laakkonen, J.P., Hyöty, H., and Vihinen-Ranta, M. (2011). Coxsackievirus B3-induced cellular protrusions: structural characteristics and functional competence. J. Virol. *85*, 6714–6724.

Petersen, T.N., Brunak, S., von Heijne, G., and Nielsen, H. (2011). SignalP 4.0: discriminating signal peptides from transmembrane regions. Nat. Methods *8*, 785–786.

Pinkert, S., Klingel, K., Lindig, V., Dorner, A., Zeichhardt, H., Spiller, O.B., and Fechner, H. (2011). Virus-host coevolution in a persistently coxsackievirus B3-infected cardiomyocyte cell line. J. Virol. *85*, 13409–13419.

Richardson, S.J., Willcox, A., Bone, A.J., Foulis, A.K., and Morgan, N.G. (2009). The prevalence of enteroviral capsid protein vp1 immunostaining in pancreatic islets in human type 1 diabetes. Diabetologia *52*, 1143–1151.

Ramond, C., Glaser, N., Berthault, C., Ameri, J., Kirkegaard, J.S., Hansson, M., Honoré, C., Semb, H., and Scharfmann, R. (2017). Reconstructing human pancreatic differentiation by mapping specific cell populations during development. Elife *6*, e27564.

Richardson, S.J., Leete, P., Bone, A.J., Foulis, A.K., and Morgan, N.G. (2013). Expression of the enteroviral capsid protein VP1 in the islet cells of patients with type 1 diabetes is associated with induction of protein kinase R and downregulation of Mcl-1. Diabetologia *56*, 185–193.

Robinson, S.M., Tsueng, G., Sin, J., Mangale, V., Rahawi, S., McIntyre, L.L., Williams, W., Kha, N., Cruz, C., Hancock, B.M., et al. (2014). Coxsackievirus B exits the host cell in shed microvesicles displaying autophagosomal markers. PLoS Pathog. *10*, e1004045.

Ryall, C.L., Viloria, K., Lhaf, F., Walker, A.J., King, A., Jones, P., Mackintosh, D., McNeice, R., Kocher, H., Flodstrom-Tullberg, M., et al. (2014). Novel role for matricellular proteins in the regulation of islet β cell survival: the effect of SPARC on survival, proliferation, and signaling. J. Biol. Chem. *289*, 30614–30624.

Sane, F., Caloone, D., Gmyr, V., Engelmann, I., Belaich, S., Kerr-Conte, J., Pattou, F., Desailloud, R., and Hober, D. (2013). Coxsackievirus B4 can infect human pancreas ductal cells and persist in ductal-like cell cultures which results in inhibition of Pdx1 expression and disturbed formation of islet-like cell aggregates. Cell. Mol. Life Sci. *70*, 4169–4180.

Sean, P., Nguyen, J.H.C., and Semler, B.L. (2009). Altered interactions between stem-loop IV within the 5′ noncoding region of coxsackievirus RNA and poly(rC) binding protein 2: effects on IRES-mediated translation and viral infectivity. Virology *389*, 45–58.

Sin, J., McIntyre, L., Stotland, A., Feuer, R., and Gottlieb, R.A. (2017). Coxsackievirus B escapes the infected cell in ejected mitophagosomes. J. Virol. *91*, e01347–17.

Sioofy-Khojine, A.B., Lehtonen, J., Nurminen, N., Laitinen, O.H., Oikarinen, S., Huhtala, H., Pakkanen, O., Ruokoranta, T., Hankaniemi, M.M., Toppari, J., et al. (2018). Coxsackievirus B1 infections are associated with the initiation of insulin-driven autoimmunity that progresses to type 1 diabetes. Diabetologia *61*, 1193–1202.

Song, L., and Fricker, L.D. (1995). Calcium- and pH-dependent aggregation of carboxypeptidase E. J. Biol. Chem. *270*, 7963–7967.

Tapparel, C., Siegrist, F., Petty, T.J., and Kaiser, L. (2013). Picornavirus and enterovirus diversity with associated human diseases. Infect. Genet. Evol. *14*, 282–293.

Tuthill, T.J., Groppelli, E., Hogle, J.M., and Rowlands, D.J. (2010). Picornaviruses. Curr. Top. Microbiol. Immunol. *343*, 43–89.

Vizcaíno, J.A., Côté, R.G., Csordas, A., Dianes, J.A., Fabregat, A., Foster, J.M., Griss, J., Alpi, E., Birim, M., Contell, J., et al. (2012). The Proteomics Identifications (PRIDE) database and associated tools: status in 2013. Nucleic Acids Res. *41*, D1063–D1069.

Wai, T., and Langer, T. (2016). Mitochondrial dynamics and metabolic regulation. Trends Endocrinol. Metab. *27*, 105–117.

Xu, J., Nie, H., Zhang, X., Tian, Y., and Yu, B. (2011). Down-regulated energy metabolism genes associated with mitochondria oxidative phosphorylation and fatty acid metabolism in viral cardiomyopathy mouse heart. Mol. Biol. Rep. *38*, 4007–4013.

Ylipaasto, P., Klingel, K., Lindberg, A.M., Otonkoski, T., Kandolf, R., Hovi, T., and Roivainen, M. (2004). Enterovirus infection in human pancreatic islet cells, islet tropism in vivo and receptor involvement in cultured islet beta cells. Diabetologia *47*, 225–239.

Ylipaasto, P., Kutlu, B., Rasilainen, S., Rasschaert, J., Salmela, K., Teerijoki, H., Korsgren, O., Lahesmaa, R., Hovi, T., Eizirik, D.L., et al. (2005). Global profiling of coxsackievirus- and cytokine-induced gene expression in human pancreatic islets. Diabetologia *48*, 1510–1522.

Ylipaasto, P., Smura, T., Gopalacharyulu, P., Paananen, A., Seppanen-Laakso, T., Kaijalainen, S., Ahlfors, H., Korsgren, O., Lakey, J.R., Lahesmaa, R., et al. (2012). Enterovirus-induced gene expression profile is critical for human pancreatic islet destruction. Diabetologia *55*, 3273–3283.

Yoon, J.W., Austin, M., Onodera, T., and Notkins, A.L. (1979). Isolation of a virus from the pancreas of a child with diabetic ketoacidosis. N. Engl. J. Med. *300*, 1173–1179.

Yu, C.-Y., Liang, J.-J., Li, J.-K., Lee, Y.-L., Chang, B.-L., Su, C.-I., Huang, W.-J., Lai, M.M.C., and Lin, Y.-L. (2015). Dengue virus impairs mitochondrial fusion by cleaving mitofusins. PLoS Pathog. *11*, e1005350.

Zhang, H.M., Ye, X., Su, Y., Yuan, J., Liu, Z., Stein, D.A., and Yang, D. (2010). Coxsackievirus B3 infection activates the unfolded protein response and induces apoptosis through downregulation of p58IPK and activation of CHOP and SREBP1. J. Virol. *84*, 8446–8459.

Zhao, X., Zhang, G., Liu, S., Chen, X., Peng, R., Dai, L., Qu, X., Li, S., Song, H., Gao, Z., et al. (2019). Human neonatal fc receptor is the cellular uncoating receptor for enterovirus B. Cell *177*, 1553–1565.e16.

**ISCI, Volume *19***

## Supplemental Information

# Coxsackievirus B Persistence Modifies the Proteome and the Secretome of Pancreatic Ductal Cells

**Niina Lietzén, Karoliina Hirvonen, Anni Honkimaa, Tanja Buchacher, Jutta E. Laiho, Sami Oikarinen, Magdalena A. Mazur, Malin Flodström-Tullberg, Eric Dufour, Amir-Babak Sioofy-Khojine, Heikki Hyöty, and Riitta Lahesmaa**

Figure S1 (related to Fig. 7). IFNL1 RT-qPCR for cells cultured in serum-containing medium.

A sample set including three biological repeats of persistently infected cells and non-infected cells in serum-containing medium were collected at 279, 286 and 293 days post infection for innate immune response analysis similarly as described in Materials and Methods-section, but the cells were lysed and stored in RLT-lysis buffer prior to RNA extraction.

IFNL1 mRNA was quantified using the Taqman Gene expression assay (Applied Biosystems). In brief, extracted RNA (RNeasy kit, Qiagen) was transcribed into cDNA using random hexamers, dNTP mix, RNase inhibitor and 5x Buffer (Promega). PCR reaction was performed using TaqMan® Fast Advanced Master Mix (Applied Biosystems) and human specific Gene expression assay primer/probe set (Applied Biosystems) to amplify and quantify human IFNL1 (Assay ID: Hs00601677_g1). Samples were run on a QuantStudio5 (Applied Biosystems) Comparative Ct Fast program (20 sec of 95°C followed by 40 cycles of 1 sec 95°C, 20 sec 60°C). All reactions were performed in triplicate and gene expression of the studied genes was normalized to the reference gene (GAPDH) and expressed as deltaCt.

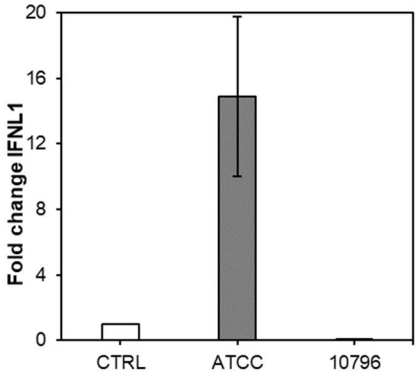

Table S1 (related to Fig. 1). Evaluation of cell death.

Cell death was approximated by ToxiLight cell viability assay kit. Samples from the first two timepoints used for proteomics analyses (#1 and #2) were analysed. The measurements were performed after culturing the cells in FBS-free medium for two days. Minor (<10 %) cell death was detected at each sample. CVB1 ATCC samples marked with an asterisk (*) are test samples in which the two days culture in serum-free medium (#1) was compared with 5 days culture in serum-free medium (#2). No significant difference was detected.

| Sample | Cell death percentage (n=3) |
|---|---|
| control #1 | 5.40 ± 0.14% |
| control #2 | 8.00 ± 0.53 % |
| CVB1 ATCC #1 | 3.52 ± 0.14 % |
| CVB1 ATCC #2 | 5.66 ± 0.34% |
| CVB1 10796 #1 | 1.31 ± 0.06 % |
| CVB1 10796 #2 | 2.02 ± 0.10 % |
| CVB1 ATCC #1 * | 4.11 ± 0.31 % |
| CVB1 ATCC #2 * | 4.27± 0.47 % |

Table S6 (related to Fig. 3 and Fig. 5). Gene Ontology (cellular component) enrichment of the differentially expressed proteins in (A) cell lysates and (B) secretome using DAVID tool. Only significantly enriched categories (FDR < 0.05) are shown.

A

| Upregulated in cells during persistent CVB1 ATCC infection | | | |
|---|---|---|---|
| Term | Count | Fold Enrichment | FDR |
| GO:0005737~cytoplasm | 203 | 1.315252 | 1.90E-04 |
| GO:0005829~cytosol | 167 | 1.317985 | 0.008838 |
| | | | |
| Upregulated in cells during persistent CVB1 CDC7 infection | | | |
| Term | Count | Fold Enrichment | FDR |
| GO:0005829~cytosol | 169 | 1.358935 | 7.60E-04 |
| GO:0005634~nucleus | 182 | 1.330353 | 8.18E-04 |
| | | | |
| Downregulated in cells during persistent CVB1 ATCC infection | | | |
| Term | Count | Fold Enrichment | FDR |
| GO:0016021~integral component of membrane | 224 | 1.397357 | 4.47E-06 |
| GO:0005753~mitochondrial proton-transporting ATP synthase complex | 14 | 5.059959 | 5.61E-05 |
| GO:0005759~mitochondrial matrix | 65 | 1.685573 | 0.015347 |
| | | | |
| Downregulated in cells during persistent CVB1 10796 infection | | | |
| Term | Count | Fold Enrichment | FDR |
| GO:0005739~mitochondrion | 366 | 1.407814 | 1.18E-14 |
| GO:0005759~mitochondrial matrix | 124 | 1.715361 | 9.74E-10 |
| GO:0005743~mitochondrial inner membrane | 159 | 1.567081 | 8.79E-09 |
| GO:0016021~integral component of membrane | 389 | 1.294519 | 1.84E-08 |
| GO:0005765~lysosomal membrane | 68 | 1.565463 | 0.021283 |
| | | | |

B

| Top 20 Gene Ontology classes enriched among the differentially expressed proteins in secretome data | | | |
|---|---|---|---|
| Term | Count | Fold Enrichment | FDR |
| GO:0070062~extracellular exosome | 623 | 2.779747149 | 2.54E-150 |
| GO:0005829~cytosol | 505 | 1.910671114 | 7.62E-53 |
| GO:0005913~cell-cell adherens junction | 127 | 4.93150288 | 2.76E-52 |
| GO:0005925~focal adhesion | 139 | 4.458780933 | 2.50E-51 |
| GO:0016020~membrane | 370 | 2.109391228 | 1.00E-45 |
| GO:0005737~cytoplasm | 617 | 1.481925561 | 7.19E-29 |
| GO:0031012~extracellular matrix | 87 | 3.686426964 | 4.62E-24 |
| GO:0043202~lysosomal lumen | 45 | 6.640055058 | 4.41E-23 |
| GO:0022625~cytosolic large ribosomal subunit | 38 | 7.008947006 | 3.97E-20 |
| GO:0005840~ribosome | 59 | 4.457814741 | 5.08E-20 |
| GO:0005615~extracellular space | 206 | 1.918128583 | 1.18E-17 |
| GO:0005764~lysosome | 60 | 3.329821121 | 1.67E-13 |
| GO:0005654~nucleoplasm | 332 | 1.495708443 | 3.23E-12 |
| GO:0042470~melanosome | 35 | 4.346350671 | 2.12E-10 |
| GO:0005730~nucleolus | 129 | 1.887934752 | 2.71E-09 |
| GO:0005788~endoplasmic reticulum lumen | 48 | 3.135581555 | 3.30E-09 |
| GO:0048471~perinuclear region of cytoplasm | 101 | 2.039895247 | 1.06E-08 |
| GO:0030529~intracellular ribonucleoprotein complex | 38 | 3.504473503 | 2.63E-08 |
| GO:0005794~Golgi apparatus | 126 | 1.831208695 | 4.17E-08 |
| GO:0009986~cell surface | 86 | 1.990110803 | 1.60E-06 |

Table S7 (related to Fig. 5 and Fig. 7). Reagents used for RT-qPCR.

| Gene | 1) 5' -PROBE- 3'<br>2) 5' -PRIMER 1- 3'<br>3) 5' -PRIMER 2 -3' |
|---|---|
| CHGB | 1) Universal Probelibrary probe #79<br>2) 5'- ttctgaggagccggtgag -3'<br>3) 5'- gaactcgaaaacttggctgc -3' |
| CPE | 1) Universal Probelibrary probe #3<br>2) 5'- gaaagtggcagttccttacagc -3'<br>3) 5'- ttttgaactggagtcattttctga -3' |
| IFNL1 | 1) Universal Probelibrary probe #79<br>2) 5' - ggcctgtatccagcctca -3'<br>3) 5' - ctggaggcatctgtcacctt- 3' |
| SCG3 | 1) Universal Probelibrary probe #47<br>2) 5'- gagtggattggatcataaatttcaa -3'<br>3) 5'- atgaagtagcagaggttttacaaaaat -3' |

TRANSPARENT METHODS

## Establishment of persistent enterovirus infection in PANC-1 cells

Pancreatic ductal cells (PANC-1 cell line obtained from Professor Didier Hober's laboratory, Lille, France) were cultured in Dulbecco's modified eagles media (DMEM) supplemented with 10 % v/v of fetal bovine serum (FBS, Gibco) and 0.5 % v/v penicillin- streptomycin (Pen-Strep, Gibco). Persistent infection was established using a protocol earlier published by Famara Sane and the colleagues (Sane et al., 2013). PANC-1 cells were infected with CVB1 prototype strain obtained from ATCC (American type culture collection, strain Conn-5) and with a wild type CVB1 strain (strain 10796), which was obtained from Centers for Disease Control and Prevention (CDC) and isolated originally in Argentina in 1983 (Hamalainen et al., 2014). Primary infection of PANC-1 cells was done using a low titer of the virus leading to a strong cytopathic effect and extensive cell death. After 11 days post infection all remaining living cells were detached from the plastic mechanically by scraping with cell scraper (Greiner Bio-One) and transferred on fresh PANC-1 cells in a 6-well plate (Nunc). A strong cytopathic effect was again seen soon after the cells were added on top of fresh cells, after which the remaining living cells were maintained by washing the culture plates with Hank's balanced salt solution (HBSS) regularly. After the cells started to grow they were maintained by regular HBSS washes and passaged once a week by using cell scraper. The presence of the virus in the persistent infection models was verified by RT-qPCR method earlier described by Honkanen et al. (Honkanen et al., 2013), which detects the viral RNA from culture supernatants. In addition, viral protein VP1 was detected from cellular samples by IHC (see below). Plaque morphology of the virus was verified by standard plaque titration assay on GMK cells. Resistance of persistently infected cells to coinfection with the parental virus strain and CVB3 (obtained from ATCC) was carried out as described earlier (Alidjinou et al., 2017; Pinkert et al., 2011).

## Detection of viral protein by immunohistochemistry

The cells were harvested 362 days post infection by scraping and fixed in 10% formalin (Oy FF-Chemicals Ab) for 24 h prior to dehydration and paraffin embedding. An automated immunostaining was performed for the formalin-fixed paraffin-embedded (FFPE) cell samples using a commercially available monoclonal antibody (clone 5-D8/1, Agilent Dako, product code M 7064), detecting enterovirus capsid protein VP1, as previously described (Krogvold et al., 2015). Imaging was done using an Olympus BX-60 microscope.

## Sample collection for proteomics

Three biological repeats of persistently infected cells and non-infected control cells were collected 300-322 days post infection for proteomics analysis. The cells were cultured in serum-free DMEM medium supplemented with antibiotics for four days prior to sample collection. Cells were collected by scraping (Grainer-Bio cell scraper), pelleted by centrifugation for 2500 rpm, 10min (Heraeus Christ) and frozen as dry cell pellets in -80 ˚C. Cell culture supernatants were also collected, cleared by centrifugation (Heraeus Christ centrifuge, 2500 rpm, 10min) and stored at -80 °C. Cell viability in proteomics samples was estimated two days prior to sample collection by ToxiLight™ Non-destructive Cytotoxicity BioAssay Kit (Lonza) by following the kit instructions (Table S1).

Cell lysis and digestion by FASP

The cell pellets were lysed in 200 µl of 4 % SDS and 0.1 M dithiothreitol (DTT) in 0.1 M Tris HCl, pH 7.6. First, the samples were incubated at 95 °C for 5 min to inactivate the virus and to denature the proteins, followed by a sonication step to reduce the viscosity of the cell pellet. The samples were then centrifuged at 16 000 x g at 20 °C for 20 min, and the supernatant containing the extracted proteins was collected. For detergent removal and protein digestion slightly modified filter assisted sample preparation (FASP) protocol was used (Wiśniewski et al., 2009). Around 60 µg of protein lysate was added in Microcon-30 kDa filter units YM-30 (Millipore). Then 400 µl of 8 M urea in 0.1 M Tris/HCl, ph 8.5 (UA) was added to each filter and centrifuged at 8 000 x g at 20 °C for 25 min. This step was repeated twice. Right after, 300 µl of 0.05 M iodoacetamide (IAA) in UA was added to each filter and were incubated in dark for 20 min. The filters were then washed twice with 400 µl of UA by centrifuging the samples at 8 000 x g at 20 °C for 30 min. The buffer was then changed to digestion buffer by centrifuging twice with 400 µl of 10 % acetonitrile in 25 mM Tris/HCl, pH 8.0 at 8 000 x g at 20 °C for 30 min. Trypsin (Promega) was then added to each filter with 300 µl of digestion buffer. The used enzyme-protein ratio was 1:30. The samples were incubated overnight at 37 °C and the peptides were collected in the following day by centrifuging at 8 000 x g at 20 °C for 10 min that was followed by a rinsing step by centrifuging 250 µl of digestion buffer at 8 000 x g at 20 °C for 30 min. The samples were then dried and reconstituted for desalting with 1 ml of 0.1 % TFA. The desalting step was performed with Sep-Pak® C18 96-well plate (Waters) after which the samples were dried using a speed vacuum centrifuge. For the MS analyses, the dried samples were dissolved into 2 % FA 2 % ACN and the protein concentration was determined using NanoDrop-1000 UV-spectrometer (Thermo Scientific). Approximately 250 ng of each sample was injected to LC-MS/MS analysis. All samples were analyzed in technical triplicates in a randomized order.

Cell culture supernatant digestion

First, 7 ml of cell culture media for each sample was concentrated in 10 kDa Amicon Ultra-15 Centrifugal filter units (Merck Millipore) (3 220 g at 4 °C for 1h). The concentrated samples were collected and heated at 95 °C for 5 min to inactivate the virus. The samples were then further concentrated by using 3 kDa Amicon Ultra-0.5 Centrifugal filter units (Merck Millipore) (14 000 x g at 20 °C for 1 h). Right after, 250 µl of 8 M urea in 0.1 M ammonium bicarbonate (AmBic) was added to the filters and centrifuged at 14 000 x g at 20 °C for 45 min to change the buffer. The remaining sample inside the filter unit was collected and transferred to a new tube. The disulphide bonds were then reduced by adding 5 mM final concentration of DTT in 0.1 M AmBic and incubating the samples at 37 °C for 1h. Subsequently, an alkylation step was performed by adding 13 mM final concentration of 1 M IAA in 0.1 M AmBic to each sample and incubating the samples in dark at room temperature for 30 min. The urea concentration in each sample was decreased below 1.5 M by adding 0.1 M AmBic. To each sample we added around 1:20 enzyme-substrate ratio of trypsin (Promega) and incubated the samples at 37 °C overnight. In the following day the trypsin activity was stopped by reducing the pH below pH 3. The samples were then desalted using Sep-Pak® C18 cartridges (Waters) and dried in a speed vacuum centrifuge. The dried samples were then reconstituted and the protein amount was determined as described in the previous section. The loading and LC-MS/MS analysis were likewise done as described earlier.

Mass spectrometric analyses

The peptide samples were measured by Q Exactive™ HF Hybrid Quadrupole-Orbitrap™ mass spectrometer (Thermo Fischer Scientific) that was interfaced with EASY-nLC 1200 liquid chromatograph (Thermo Fischer Scientific) and a nano-electrospray ion source (Thermo Fischer Scientific). The peptides were directly loaded into an in-house packed 40 cm 75 µm ID capillary column with 1.9 µm Reprosil-Pur $C_{18}$ beads (Dr. Maisch) in buffer A (0.1 % (v/v) formic acid). Subsequently, the peptides were separated using a 110-min gradient starting from linear 75-min gradient of 7-25 % of buffer B (0.1 % (v/v) formic acid, 80 % (v/v) acetonitrile), followed by 15-min increase to 35 % of buffer B and then 10-min increase to 100 % of buffer B before 10-min washing step with 100 % buffer B. The column temperature was kept at 60 °C throughout the runs using an in-house column oven. The full scan resolution was set to 120 000 at m/z 200 and the MS spectra were collected in the 300-1700 m/z range with an ion target value of $3 \times 10^6$ and maximum injection time of 100 ms. The 12 most intense precursors were selected for fragmentation that was performed by high energy C-trap dissociation (HCD) with a normalized collision energy of 27 eV. MS2 scans were performed at a resolution of 15 000 at m/z 200, in the range 200-2000 m/z for 200 ms and with an ion target value of $5 \times 10^4$. To avoid repeated selection of precursor ions dynamic exclusion was set to 20 s.

Proteomics data processing and statistical analysis

MaxQuant software (Cox and Mann, 2008) version 1.5.5.1 was used for a data processing of the raw MS files obtained from the LC-MS/MS analyses. The in-built Andromeda search engine (Cox et al., 2011) was used to search the peptide lists against a combined database of SwissProt human and TrEMBL enterovirus sequences (version June 2018, 80862 entries) with added iRT peptide sequences and a common contaminants database. Label-free quantification was performed with the LFQ ratio count of 2. N-terminal acetylation and methionine oxidation was used as a variable modifications and cysteine carbamidomethylation as a fixed modification. For both proteins and peptides the false discovery rate (FDR) was set to 1 % and was determined by searching a reverse database. The minimum peptide length was set to seven amino acids. The enzyme specificity was set to trypsin and the maximum number of allowed missed cleavages was two. In order to transfer the peptide identification across the raw files a “match between runs” feature was used. Otherwise the default settings were used.

The processed data from MaxQuant was analyzed with Perseus software (Tyanova et al., 2016) using the normalised LFQ intensities. First, proteins identified only based on modified peptides and identifications from the reversed decoy database removed, followed by manual removal of potential contaminant proteins not present in the used human and enterovirus sequence database. Also, minimum two razor and/or unique peptide identifications were required for each protein. The median LFQ intensities of the three technical replicates were calculated with the requirement of minimum of two valid values per sample. Finally, only proteins quantified in at least three samples were kept.

Unpaired Student’s t-test implemented in Perseus (Tyanova et al., 2016) was applied to identify differentially expressed proteins. Proteins with false discovery rate (FDR) < 5 % and |fold-change| > 1.5 were considered significantly differentially expressed.

## Quantitative real time-PCR

Total RNA was extracted using the AllPrep DNA/RNA/miRNA Universal Kit (Qiagen) and treated in-column with DNase (RNase-Free Dnase Set; QIAGEN) for 15 minutes. The removal of genomic DNA was ascertained by treating the samples with DNase I (Invitrogen) before cDNA synthesis with SuperScript II Reverse Transcriptase (Invitrogen). Quantitative real time-PCR (qPCR) was performed using KAPA™ probe fast qPCR Master Mix (Kapa Biosystems) and Universal ProbeLibrary probes (Roche Applied Science) with custom ordered primers (Table S7). The qPCR runs were analyzed with Applied Biosystems QuantStudio 12K Flex Real-Time PCR System (10 minutes enzyme activation and 40 cycles of 15 sec 95°C, 1 min 60°C). All reactions were performed in triplicate. The cycle threshold (Ct) values of the target transcripts were normalized against the signal acquired with GAPDH (housekeeping gene) and expressed as deltaCt = ($Ct_{Gene}$–$Ct_{GAPDH}$).

## Detection of IFIH1 expression by in situ hybridization

A commercial QuantiGene ViewRNA in situ hybridization –technique was applied to detect a viral pattern recognition receptor IFIH1/MDA5 (#VA1-13031) in FFPE samples. These FFPE samples were collected from two different time points (102 days and 228 days post infection). A standard protocol, according to the manufacturer's instructions was performed, as previously described (Laiho et al., 2015). Briefly, FFPE samples were deparaffinized, dehydrated and rehydrated, followed by a 10 min boiling and a 10 min proteinase step. Targets were hybridized for 2 hrs at RT. Target-specific hybridization was followed by signal amplification using specific oligonucleotides conjugated to alkaline phosphatase. Fast Red substrate was used for detection under both bright-field and fluorescent lights. Imaging was done using Olympus BX-60 microscope.

## Mitochondrial visualization

Mitochondrial network morphology was visualized from live cell samples of persistently infected cells and non-infected control cells. Prior to the mitochondrial staining the live cells were plated on cover slip Petri dish, pre-coated with 2% gelatin (Sigma-Aldrich). Mitochondria of live persistently infected cells were stained with Mitotracker Red CMXRos (Life Technologies), which accumulates in the organelle based on the membrane potential. Mitotracker was dissolved into DMSO to prepare a 40 µM stock solution. Mitotracker stock solution was further diluted into complete DMEM, to obtain a final concentration of 20 nM; and incubated with the cells for 45 min at 37 ˚C and 5% CO2. The dye was removed by rinsing with PBS. Imaging was done using a Olympus IX51 Fluorescence Microscope. Three biological repeats of CVB1 ATCC persistent infection model and four biological repeats of non-infected control cells and CVB1 10796 persistent infection model were imaged. From each sample set, ten images were captured and analyzed. The cells were divided into four categories based on their mitochondrial network morphology. The categories were elongated filaments, filaments, intermediate and fragmented network. Elongated filaments category included cells with long filaments as mitochondrial network. Filaments category included all cells with shorter filamentous mitochondrial network but with very low to no fragmented mitochondria. Intermediate category included cells with a clear mixture of elongated and fragmented mitochondria. Fragmented category included cells with large majority of fragmented mitochondrial network. Additionally, out focused cells and uncategorized cells were included in the analysis while not included in the data presented in the figures. Uncategorized cells covered 15% of uninfected control cells, 3% of CVB1 infected cells and 4% CVB1 10796 infected cells. Percentages of cells belonging to each category were calculated for each

biological repeat, and average and standard deviations of these were calculated separately for each condition. Statistical significance was estimated using Z-test.

### Western blot analyses

Western blot analyses were performed using the same cell lysates that were used for the proteomics analyses. After boiling the samples with 6× loading dye (330 mM Tris-HCl, pH 6.8; 330 mM SDS; 6% β-ME; 170 μM bromophenol blue; 30% glycerol), the samples were loaded on Mini-PROTEAN TGX Precast Protein Gels (BioRad Laboraotries) and transferred to PVDF membranes (Trans-Blot Turbo Transfer Packs, BioRad Laboratories). The primary antibodies used: eIF4G (#2617, Cell Signaling Technologies) and beta-actin (A5441, Sigma-Aldrich).

### Functional data analyses

Functional enrichment analyses were performed using DAVID Functional Annotations (Huang et al., 2009) and Ingenuity Pathway Analysis (IPA, www.qiagen.com/ingenuity, Qiagen) tools. Gene Ontology classes with DAVID FDR <0.05 and IPA pathways with p-value <0.01 were considered as significantly enriched.

### SignalP

A neural network based SignalP (version 4.1) software was used to predict proteins with a secretory signal peptide (Petersen et al., 2011). Both SignalP-TM and SignalP-noTM networks were used to distinguish between signal peptides and transmembrane regions.

### Data availability

The raw mass spectrometry data have been deposited to the ProteomeXchange Consortium (http://proteomecentral.proteomexchange.org) via the PRIDE partner repository (Vizcaíno et al., 2012) with the dataset identifiers PXD012153 and PXD012154.

TRANSPARENT METHODS REFERENCES

Alidjinou, E.K., Engelmann, I., Bossu, J., Villenet, C., Figeac, M., Romond, M.B., Sane, F., and Hober, D. (2017). Persistence of Coxsackievirus B4 in pancreatic ductal-like cells results in cellular and viral changes. Virulence 8, 1229–1244.

Cox, J., and Mann, M. (2008). MaxQuant enables high peptide identification rates, individualized p.p.b.-range mass accuracies and proteome-wide protein quantification. Nat. Biotechnol. 26, 1367–1372.

Cox, J., Neuhauser, N., Michalski, A., Scheltema, R.A., Olsen, J. V, and Mann, M. (2011). Andromeda: a peptide search engine integrated into the MaxQuant environment. J. Proteome Res. 10, 1794–1805.

Hamalainen, S., Nurminen, N., Ahlfors, H., Oikarinen, S., Sioofy-Khojine, A.B., Frisk, G., Oberste, M.S., Lahesmaa, R., Pesu, M., and Hyoty, H. (2014). Coxsackievirus B1 reveals strain specific differences in plasmacytoid dendritic cell mediated immunogenicity. J. Med. Virol. 86, 1412–1420.

Honkanen, H., Oikarinen, S., Pakkanen, O., Ruokoranta, T., Pulkki, M.M., Laitinen, O.H., Tauriainen, S., Korpela, S., Lappalainen, M., Vuorinen, T., et al. (2013). Human enterovirus 71 strains in the background population and in hospital patients in Finland. J. Clin. Virol. 56, 348–353.

Huang, D.W., Sherman, B.T., and Lempicki, R.A. (2009). Systematic and integrative analysis of large gene lists using DAVID bioinformatics resources. Nat. Protoc. 4, 44–57.

Krogvold, L., Edwin, B., Buanes, T., Frisk, G., Skog, O., Anagandula, M., Korsgren, O., Undlien, D., Eike, M.C., Richardson, S.J., et al. (2015). Detection of a low-grade enteroviral infection in the islets of langerhans of living patients newly diagnosed with type 1 diabetes. Diabetes 64, 1682–1687.

Laiho, J.E., Oikarinen, S., Oikarinen, M., Larsson, P.G., Stone, V.M., Hober, D., Oberste, S., Flodström-Tullberg, M., Isola, J., and Hyöty, H. (2015). Application of bioinformatics in probe design enables detection of enteroviruses on different taxonomic levels by advanced in situ hybridization technology. J. Clin. Virol. 69, 165–171.

Petersen, T.N., Brunak, S., von Heijne, G., and Nielsen, H. (2011). SignalP 4.0: discriminating signal peptides from transmembrane regions. Nat. Methods 8, 785–786.

Pinkert, S., Klingel, K., Lindig, V., Dorner, A., Zeichhardt, H., Spiller, O.B., and Fechner, H. (2011). Virus-host coevolution in a persistently coxsackievirus B3-infected cardiomyocyte cell line. J. Virol. 85, 13409–13419.

Sane, F., Caloone, D., Gmyr, V., Engelmann, I., Belaich, S., Kerr-Conte, J., Pattou, F., Desailloud, R., and Hober, D. (2013). Coxsackievirus B4 can infect human pancreas ductal cells and persist in ductal-like cell cultures which results in inhibition of Pdx1 expression and disturbed formation of islet-like cell aggregates. Cell. Mol. Life Sci. 70, 4169–4180.

Tyanova, S., Temu, T., Sinitcyn, P., Carlson, A., Hein, M.Y., Geiger, T., Mann, M., and Cox, J. (2016). The Perseus computational platform for comprehensive analysis of (prote)omics data. Nat. Methods 13, 731–740.

Vizcaíno, J.A., Côté, R.G., Csordas, A., Dianes, J.A., Fabregat, A., Foster, J.M., Griss, J., Alpi, E., Birim, M., Contell, J., et al. (2012). The Proteomics Identifications (PRIDE) database and associated tools: status in 2013. Nucleic Acids Res. 41, D1063–D1069.

Wiśniewski, J.R., Zougman, A., Nagaraj, N., and Mann, M. (2009). Universal sample preparation method for proteome analysis. Nat. Methods 6, 359–362.